ADA053164

(12)

AFGL-TR-77-0286
AIR FORCE SURVEYS IN GEOPHYSICS, NO. 380

# Modeling of the Geosynchronous Orbit Plasma Environment - Part I

HENRY B. GARRETT, Capt. USAF

14 December 1977

D D C
APR 26 1978
F

Approved for public release; distribution unlimited.

SPACE PHYSICS DIVISION PROJECT 7661
AIR FORCE GEOPHYSICS LABORATORY
HANSCOM AFB, MASSACHUSETTS 01731

AIR FORCE SYSTEMS COMMAND, USAF

Best Available Copy

Best Available Copy

This report has been reviewed by the ESD Information Office (OI) and is releasable to the National Technical Information Service (NTIS).

This technical report has been reviewed and is approved for publication.

FOR THE COMMANDER

John Howard

Chief Scientist

Qualified requestors may obtain additional copies from the Defense Documentation Center. All others should apply to the National Technical Information Service.

(9) Air Force Surveys in geophysics

Unclassified

SECURITY CLASSIFICATION OF THIS PAGE (When Data Entered)

| REPORT DOCUMENTATION PAGE | READ INSTRUCTIONS BEFORE COMPLETING FORM |
|---|---|
| 1. REPORT NUMBER (14) AFGL-TR-77-0288-PT-1, AFGL-AFSG-380-PT-1 | 3. RECIPIENT'S CATALOG NUMBER |
| 4. TITLE (and Subtitle) (6) MODELING OF THE GEOSYNCHRONOUS ORBIT PLASMA ENVIRONMENT. PART I. | 5. TYPE OF REPORT & PERIOD COVERED Scientific. Interim. |
| | 6. PERFORMING ORG. REPORT NUMBER AFSG No. 380 |
| 7. AUTHOR(s) (10) Henry B. Garrett Capt, USAF | 8. CONTRACT OR GRANT NUMBER(s) |
| 9. PERFORMING ORGANIZATION NAME AND ADDRESS Air Force Geophysics Laboratory (PHG) Hanscom AFB Massachusetts 01731 | 10. PROGRAM ELEMENT, PROJECT, TASK AREA & WORK UNIT NUMBERS 76610801 62101F |
| 11. CONTROLLING OFFICE NAME AND ADDRESS Air Force Geophysics Laboratory (PHG) Hanscom AFB Massachusetts 01731 | 12. REPORT DATE (11) 14 Dec[redacted]977 |
| | 13. NUMBER OF PAGES 46 (12) 46p. |
| 14. MONITORING AGENCY NAME & ADDRESS(if different from Controlling Office) (16) 7661 (17) 08 | 15. SECURITY CLASS. (of this report) Unclassified |
| | 15a. DECLASSIFICATION/DOWNGRADING SCHEDULE |

16. DISTRIBUTION STATEMENT (of this Report)

Approved for public release; distribution unlimited.

D D C
APR 25 1978
F

17. DISTRIBUTION STATEMENT (of the abstract entered in Block 20, if different from Report)

18. SUPPLEMENTARY NOTES

19. KEY WORDS (Continue on reverse side if necessary and identify by block number)

Spacecraft charging
Environmental modeling
Plasma interactions

20. ABSTRACT (Continue on reverse side if necessary and identify by block number)

Although the role of the environment in generating spacecraft potential variations at geosynchronous orbit is well documented, variations in the ambient environment itself have not been well-defined. Similarly, no studies of the environment have attempted an analytic formulation of the various parameters needed to model the spacecraft charging phenomenon. This paper describes the parameters needed to formulate such a model and outlines a systematic procedure for constructing a simple analytic model that includes →

DD FORM 1473 1 JAN 73 EDITION OF 1 NOV 65 IS OBSOLETE

Unclassified

SECURITY CLASSIFICATION OF THIS PAGE (When Data Entered)

409 578 JOB

Unclassified

SECURITY CLASSIFICATION OF THIS PAGE(When Data Entered)

20. Abstract (Continued)

the effects of local time and geomagnetic activity. Observational data from the ATS-5 satellite are analyzed using this procedure to give a preliminary analytic description of the geosynchronous environment in the form of a FORTRAN program.

Unclassified

SECURITY CLASSIFICATION OF THIS PAGE(When Data Entered)

# Preface

The author wishes to thank C. Pike, Maj. J. Durrett, Dr. P. Rothwell, Dr. A. Rubin, C. Purvis, Dr. W. Burke, Dr. F. Rich, Dr. S. DeForest, M. Massarro, and G. Inouye for their careful review and comments on the manuscript. Special appreciation is expressed to Dr. S. DeForest of the University of California at San Diego, for providing the data and to R. McInerney of the Air Force Geophysics Laboratory, Analysis and Simulation Branch, for preparing the data for analysis. Useful discussions and data interchange were also provided by Dr. A. Konradi of Johnson Spaceflight Center and Dr. S.-Y. Su.

White Section
Buff Section
SPECIAL

# Contents



# Illustrations

# Tables

# Modeling of the Geosynchronous Orbit Plasma Environment-Part I

## 1. INTRODUCTION

Although the role of the environment in generating spacecraft potential variations at geosynchronous orbit is well documented,[1-4*] variations in the ambient environment itself have not been well-defined. Several studies have been made of the geosynchronous environment,[5-8] but none have attempted an analytic formulation of the various parameters needed by the user community in modeling the spacecraft charging phenomenon. This initial paper describes the basic set of parameters required to formulate such a model of the ambient plasma environment and outlines a systematic procedure for constructing a simple analytic model that includes the effects of local time and geomagnetic activity. Observational data from the ATS-5 satellite are analyzed using this procedure to give a preliminary analytic description of the geosynchronous environment in the form of a FORTRAN program. Although not intended as a detailed description of the environment, the model is used in evaluating local time variations of the plasma following a plasma injection event at geosynchronous orbit (the condition most likely to foster charging).

---

(Received for publication 13 December 1977)

*Due to the number of references to be included as footnotes on this page, the reader is referred to the list of references, page 35.

## 2. PLASMA CHARACTERIZATION

The first step in constructing any model is the determination of the critical parameters necessary for description of the phenomenon. In plasma physics, classical studies have shown that to describe a plasma completely, the electric field, magnetic field, and particle distribution functions must be known. Several models of the magnetospheric electric and magnetic fields exist in the open literature so they will not be discussed here. This paper will concentrate instead on the so-called plasma distribution function – its definition, its use, and its measurement.

What is the plasma distribution function? Although in general a complex concept, the distribution function is, stripped of its physical and mathematical niceties, a function which describes how many particles exist within a tiny volume of space with a velocity in a certain direction. Turning briefly to the mathematical details, one notes that F, the distribution function, is given by:

$$F(X, Y, Z, V_X, V_Y, V_Z) \qquad (1)$$

such that

$$F(X, Y, Z, V_X, V_Y, V_Z)\, dx\, dy\, dz\, dv_x\, dv_y\, dv_z$$

is the number of particles in the velocity space

$dv_x\, dv_y\, dv_z$ and spatial volume $dx\, dy\, dz$

where

$X, Y, Z$ = spatial coordinates

and

$V_x, V_y, V_z$ = velocity components.

If F is integrated over all velocities and positions within a given volume, the total number of particles in that volume is obtained (the analysis presented in this paper assumes a collisionless plasma with no particle sources or sinks).

For the purposes of this study, the plasma will be considered to be isotropic; that is, there are just as many particles traveling in direction X as in direction Y or Z. This simplifies the analysis greatly. (Only future study will reveal just

how good or bad such an assumption is and this factor should be kept in mind in the following.) Changing to spherical coordinates, one notes:

$$
\begin{aligned}
&F(X,\ Y,\ Z,\ V_x,\ V_y,\ V_z)\ dx\ dy\ dz\ dv_x\ dv_y\ dv_z \\
&\quad = f(X,\ Y,\ Z,\ v)\ dx\ dy\ dz\ v^2 \sin\theta_v\ d\theta_v\ d\phi_v\ dv \qquad (2) \\
&\quad = f(X,\ Y,\ Z,\ v)\ dx\ dy\ dz\ (4\pi v^2\ dv)
\end{aligned}
$$

where

$v = (v_x^2 + v_y^2 + v_z^2)^{1/2}$

$\theta_v, \phi_v$ = angular coordinates of the velocity vector

$f$ = isotropic distribution function

And we have integrated over $\theta_v$ and $\phi_v$:

$$\int_0^{2\pi} d\phi_v \int_0^{\pi} \sin\theta_v\ d\theta_v = 4\pi \qquad (3)$$

A commonly encountered distribution function is the so-called Maxwellian distribution:

$$f(v_i) = n_i\left(\frac{m_i}{2\pi kT_i}\right)^{3/2} e^{-m_i v_i^2/2kT_i} \qquad (4)$$

where

$n_i$ = number density of species i

$m_i$ = mass of species i

$T_i$ = temperature of species i

$v_i$ = velocity of i species

$k$ = Boltzmann constant

$f$ = distribution function in $sec^3/km^6$

Although most plasma distributions in space are neither Maxwellian nor isotropic, these assumptions are commonly made in characterizing a plasma, in order to reduce the number of parameters necessary for description. Further, Eq. (4) can be used in the calculation of the first four plasma moments that will generate the model. For a Maxwellian particle distribution, they are:

$$\langle n_i \rangle = 4\pi \int_0^\infty (v^0) f_i v^2 \, dv = n_i \tag{5}$$

$$\langle NF_i \rangle = \int_0^\infty (v^1) f_i v^2 \, dv = \frac{n_i}{2\pi} \left( \frac{2kT_i}{\pi m_i} \right)^{1/2} \tag{6}$$

$$\langle P_i \rangle = 4\pi \left( \frac{1}{3} m_i \right) \int_0^\infty (v^2) f_i v^2 \, dv = n_i kT_i \tag{7}$$

$$\langle EF_i \rangle = \left( \frac{1}{2} m_i \right) \int_0^\infty (v^3) f_i v^2 \, dv = \frac{m_i n_i}{2} \left( \frac{2\,kT_i}{\pi m_i} \right)^{3/2} \tag{8}$$

where

$\langle n_i \rangle$ = number density for species i (number/cm$^3$)

$\langle NF_i \rangle$ = number flux for species i (number/cm$^2$ sec-sr)

$\langle P_i \rangle$ = pressure for species i (dynes/cm$^2$)*

$\langle EF_i \rangle$ = energy flux for species i (ergs/cm$^2$ sec-sr)

The use of moments is simil · to expanding a function in a Taylor series. The moments are, in statistical terms, the expectation values of a variable, that is, the average value, the standard deviation, and so on). For a plasma, the moments of the velocity are taken as follows: $\langle v^0 \rangle$, $\langle v^1 \rangle$, $\langle v^2 \rangle$, and $\langle v^3 \rangle$. In Eqs. (5), (6), (7) and (8), these moments have been multiplied by constants to give physically meaningful quantities. For example, the $\langle v^2 \rangle$ moment has been multiplied by $4\pi$ and $1/3\ m_i$ to give the isotropic pressure, $4\pi(1/3\ m_i\ v^2)$.

---

*$\langle P_i \rangle$ is two-thirds of the so-called energy density which is in units of ergs/cm$^3$. The energy density is the total energy per unit volume of the plasma.

The moments, easily derived from the UCSD ATS-5 data (the instrument employed in this study), can be used to derive, a Maxwellian and a "2-Maxwellian" fit to the distribution function, as will be demonstrated.

An interesting and important feature of the four moments is that they (unlike the plasma temperature) can be averaged together to give a phy ·ically meaningful average quantity. To prove this, assume a particle distribution is given by $f_i$. Then the moments for this function are given by

$$(M)_i = \int_0^\infty M f_i v^2 \, dv$$

where M is the moment to be found for distribution i. Now assume we want to find (M) for a distribution function f where, f is the average of several distribution functions $f_i$:

$$f = \frac{1}{N} \sum_{i=1}^{N} f_i$$

Then (M) can be defined as:

$$(M) = \int_0^\infty M f v^2 \, dv$$

This gives:

$$(M) = \int_0^\infty M f v^2 \, dv = \int_0^\infty M \left( \frac{1}{N} \sum_{i=1}^{M} f_i \right) v^2 \, dv$$

$$= \frac{1}{N} \sum_{i=1}^{N} \left( \int_0^\infty M f_i v^2 \, dv \right) = \frac{1}{N} \sum_{i=1}^{N} (M)_i$$

Thus groups of the four moments can each be averaged to give a new average set of moments in a ı entirely consistent fashion. These, in turn, can be used to derive a new, averaged distribution function.

In Appendix A, it is demonstrated that if, instead of Eq. (1), the distribution function is assumed to be the sum of 2 Maxwellians or 2 plasma components for a single species i, then $n_{1i}$, $n_{2i}$, $T_{1i}$, and $T_{2i}$ can be found from Eqs. (5), (6), (7), and (8) such that:

$$f(v) = \left(\frac{m_i}{2\pi k}\right)^{3/2} \left(\frac{n_{1i}}{T_{1i}^{3/2}} e^{-m_i V^2/2kT_{1i}} + \frac{n_{2i}}{T_{2i}^{3/2}} e^{-m_i V^2/2kT_{2i}}\right) \tag{9}$$

In Figure 1 are plotted actual distribution functions, the Maxwellian fit, and the 2 Maxwellian fit. Neither exactly fits the distribution functions but, of the two approximations, the 2 Maxwellian fit gives a much better representation of the actual distribution function (for most studies of the effects of the ambient environment, a single Maxwellian has been considered adequate – clearly a dubious assumption). In this paper, the parameters necessary to compute both the single Maxwellian and 2 Maxwellian distributions will be derived. Figure 1, however, should be remembered in considering the accuracy of either representation.

The second moment, $\langle NF_i \rangle$, may be utilized in the calculation of another important quantity, the current per unit area to the spacecraft. As the charge striking a unit area of the spacecraft per unit time is of concern, the vector velocity $\vec{v}_i$ relative to the unit normal n to the surface must be taken into account. Also, only particles entering one half of the sphere (that is, particles reaching the satellite surface from one side only) are considered. Thus:

$$\begin{aligned} J_i &= q_i \int \vec{v}_i \cdot \vec{n} \, f \, d^3 v \\ &= q_i \int_0^{\pi/2} \sin\theta_v \cos\theta_v \, d\theta_v \int_0^{2\pi} d\phi_v \int_0^{\infty} f \, v^3 \, dv \\ &= \frac{q_i n_i}{2}\left(\frac{2kT_i}{\pi m_i}\right)^{1/2} = q_i \, \pi \, \langle NF_i \rangle \end{aligned} \tag{10}$$

where

$q_i$ = charge on species (coulombs)

$J_i$ = current per unit area (amps/cm$^2$).

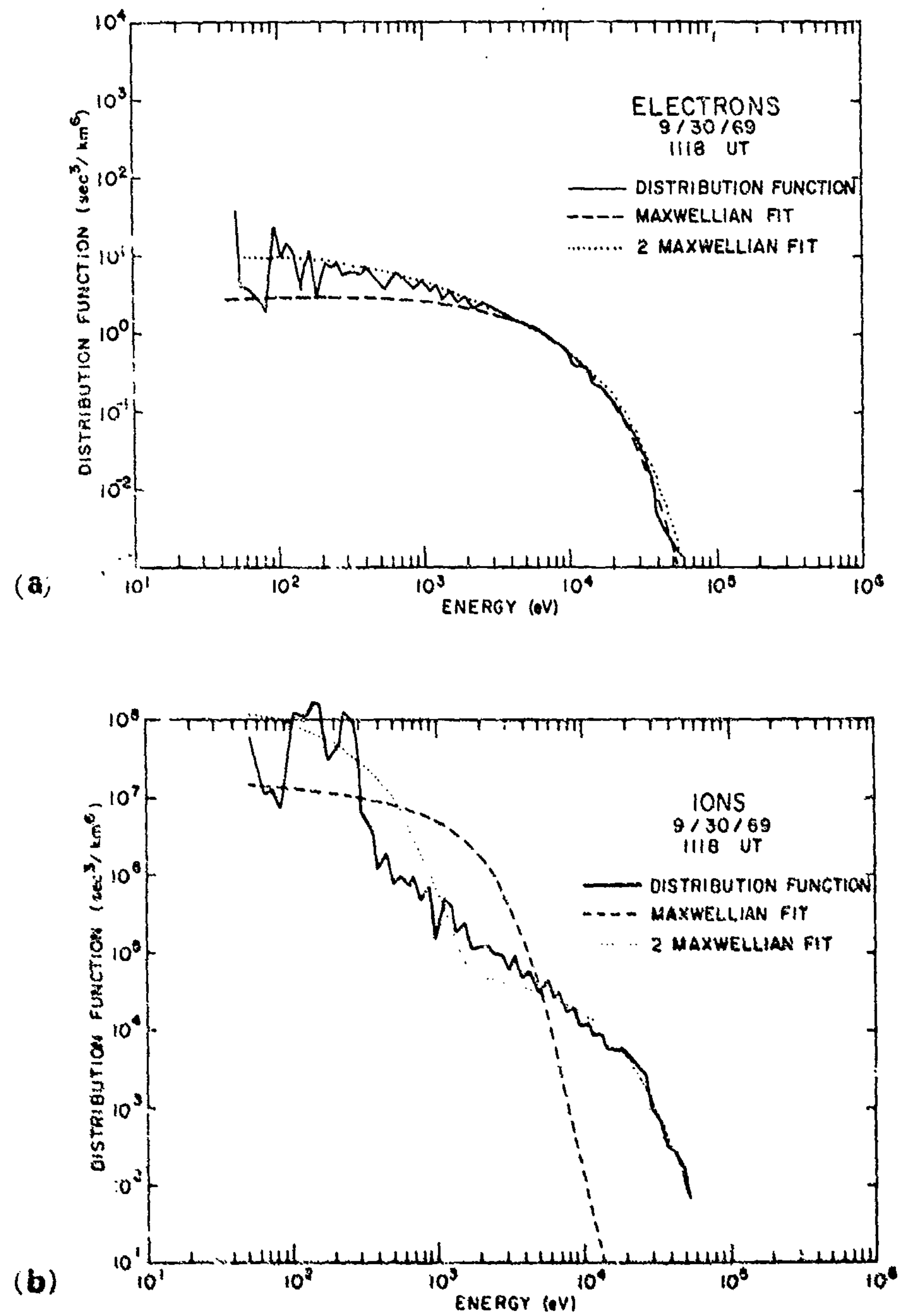


Figure 1. Actual Maxwellian Fit and 2 Maxwellian Fit Distribution Functions for 30 Sept 1969; (a) Electrons, and (b) Ions

Another quantity of general usage is the mean energy. The mean energy, $\langle E_i \rangle$ (that is, the average energy per particle), for a Maxwellian distribution is defined as the ratio of the energy density to the number density (where $\langle P_i \rangle$ is two-thirds of the energy density):

$$\langle E_i \rangle = \frac{3}{2} \langle P_i \rangle / \langle n_i \rangle = \frac{3}{2} kT_i \tag{11}$$

where $kT_i$, the quantity used in defining the Maxwellian distribution, can be obtained from $\langle E_i \rangle$ by means of this relation.

The distribution function (approximated either by a Maxwellian or, better, 2 Maxwellian fit), the mean energy, and current are the three quantities most often required by programs designed to calculate spacecraft-plasma interactions. Thus, given the four moments and Eqs. (4), (9), (10), and (11), a description of the plasma environment can be derived which meets the majority of the user community's needs.

## 3. METHOD OF ANALYSIS

In the preceding section, the parameters necessary to define the ambient plasma were described. All exhibit large temporal and spatial variations at geosynchronous orbit, making their accurate determination quite difficult. In fact, it is this extreme variation, particularly during geomagnetic storms, that has prevented analytic models from being generated. The method to be outlined is, as a result, a first-order approximation. Its usefulness can be determined only in retrospect by how well it predicts conditions at geosynchronous orbit. We can, however, describe the characteristics of a meaningful model and build those explicitly into the analysis process.

What characteristics must a model of the geosynchronous environment possess? In particular, how can the observed temporal and spatial variations be accounted for? The scale of the variations give important clues to the answer. First, changes in geomagnetic activity correlate with the largest temporal variations in the plasma. Secondly, spatial variations at geosynchronous orbit translate into local time (or position relative to the sun) variations. Thus, the two important variations are geomagnetic activity and local time.

Geomagnetic activity has been defined historically in terms of geomagnetic storms at the earth's surface.[9] These storms appear as initially small increases in the earth's horizontal magnetic field amplitude (~10 - 100 γ,

9. Rostoker, G. (1972) Geomagnetic indices, Rev. Geophys. 10(No. 4):935.

where a $\gamma$ is $10^{-5}$ of a gauss – the earth's field is $\sim 0.3$ gauss) followed by a rapid $\sim 1000\ \gamma$ decrease. This decrease may last a day or more after which the field slowly (~week) recovers to its quiet value. Such events are believed to be the result of a compression of the earth's magnetic field by the solar wind and are generally accompanied by auroral activity, ionospheric perturbations, particle fluxes at geosynchronous orbit, and so on. A typical magnetic record is shown in Figure 2.

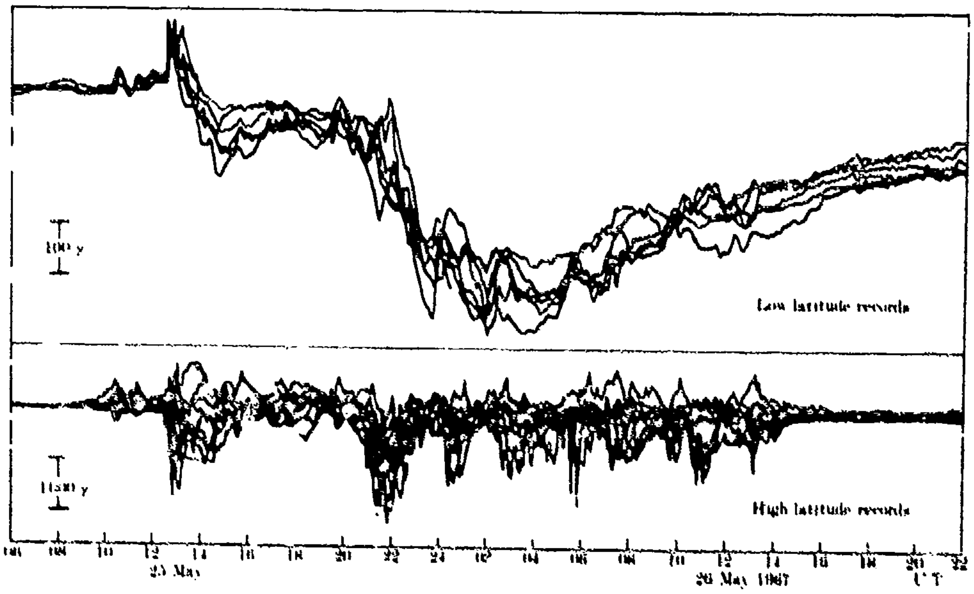


Figure 2. Example of a Geomagnetic Storm Showing the SSC (storm sudden commencement) and the Resulting Magnetic Variations at the Earth's Surface (Akasofu and Chapman, 1972)

Traditionally, the level of world-wide geomagnetic activity as represented by fluctuations in the earth's magnetic field has been defined by the 3 hour $K_p$ index which goes from 0 to 9 in steps of 1/3. This is a quasi-logarithmic quantity which is supposed to represent the positive and negative deviation of an "average" magnetometer at mid-latitudes. The $a_p$ index is directly calculated from the $K_p$ index and, when multiplied by 2 $\gamma$'s is supposed to give the magnetic deviation in $\gamma$'s.[9] These two quantities, due to the localized nature of most geomagnetic activity, are underestimates of actual geomagnetic activity. They are, however,

the only quantities currently available. In this study, $A_p$, the daily sum of $a_p$, will be employed as the index of geomagnetic activity.*

The determination of how the distribution function changes in local time and with $A_p$ is a significantly different problem from determining average conditions or extreme values. This is particularly true in a study of charge buildup for the proper relationship between $A_p$ and local time relative to the sun of the satellite and the interrelationship between parameters must be preserved simultaneously. Finally, in order to make the model of general utility, it should be expressible in an analytical form. To fulfill these requirements, a multiple linear regression analysis was carried out.

In multiple regression, the coefficients of a simple analytic expression are adjusted so that the deviations between the observed and predicted values as described by the chi-squared statistic are minimized. For this initial study, a linear relation in daily $A_p$ and a diurnal and semidiurnal variation in local time t were selected. That is, a collection of observations varying in local time and $A_p$ of a given moment were fit using the following equation:

$$M(t, A_p) = (a_o + a_1 A_p)(b_o + b_1 \cos\left[\frac{\pi}{12}(t + t_1) + b_2 \cos\left(\frac{\pi}{6}(t + t_2)\right)\right] \qquad (12)$$

where: $M(t, A_p)$ = predicted value of the moment M at local time t and for the daily geomagnetic activity index $A_p$, and $a_o$, $a_1$, $b_o$, $b_1$, $b_2$, $t_1$, $t_2$ = coefficients determined by the regression. Using a multiple regression program, from Bevington,[10] we note that $a_o$, $a_1$, $b_o$, $b_1$, $b_2$, $t_1$, and $t_2$ were determined for each set of moments, $A_p$, and t. The standard deviation for each point was assumed to be the standard deviation of each set of moments for analysis purposes.

In summary, the plasma environment at geosynchronous orbit varies with geomagnetic activity and local time (that is, the position of the satellite relative to the sun). To preserve this relationship, each parameter is fit, using multiple linear regression, to a simple function in $A_p$ and local time. Each parameter, predicted for the same value of $A_p$ and local time, can then be combined to give the distribution function and other parameters of interest. A FORTRAN listing of the resulting model is given in Appendix A.

---

10. Bevington, P. R. (1969) Data Reduction and Error Analysis for the Physical Sciences, McGraw-Hill, New York.

*$A_p$ was employed in lieu of $a_p$, as the spread in $a_p$ in the data base was inadequate in local time for meaningful comparisons. The use of $A_p$ also allows the analytic expression to include the observation that particle injections at geosynchronous orbit produce effects lasting up to 24 hours.

## 4. DATA BASE

To test the method just described, measurements made by the University of California at San Diego (UCSD) plasma experiment on ATS-5 were analyzed. In August 1969, ATS-5 was launched into geosynchronous orbit (6.6 $R_E$) near 105°W. The satellite spin period is 0.79 sec and the spin axis is aligned with that of the earth's. The UCSD instrument consists of four cylindrical plate spectrometers: two pairs of electron and positive ion detectors directed parallel and perpendicular to the spin axis. Three simultaneous measurements, 0.26 sec long, can be taken every 0.32 sec. A complete spectrum of 64 steps of energy channels (two are background, the others are each 112 percent of the previous channel starting at 51.6 eV and ending at 51.6 keV) can be taken in 20.48 sec. Other modes are possible, but for this study only two to four minute averages of the four moments of the distribution function are studied. A more detailed description of the calculation of the four moments from the UCSD data is given in Appendix A.

As the primary purpose of this paper is to outline a procedure for obtaining an analytic formulation of the geosynchronous plasma useful in studing charging effects, we do not use a large data set nor are the days selected at random (see the following). Ten days of hourly measurements were chosen which covered a wide range of geomagnetic activity. Data gaps and other singularities were ignored and interpolated values employed (even so, this involved only about 8 of the 240 observations). Table 1 lists the ten days chosen and the corresponding 3-hour $a_p$ and daily $A_p$ values (see Rostoker,[9] for a review of geomagnetic indices). Initially 250 sets of moments were selected (one set every hour on the half-hour plus the values at plasma injection, if clearly identifiable). The plasma components perpendicular and parallel to the satellite spin axis were averaged together, assuming equal weights.* Finally, to facilitate a comparison with the 3-hour $a_p$ index, 3-hour averages were taken. It was this data base of 80 values per moment which was analyzed.

The data base was not selected at random to avoid errors in the local time variations which are affected by single injection events. As discussed in DeForest and McIlwain[5] or Garrett et al,[4] an injection event is the sudden appearance of hot, plasma sheet plasma near local midnight at geosynchronous orbit. Unfortunately, these events are by their very nature random in occurrence. Such events cause order of magnitude changes in the plasma conditions at geosynchronous orbit and tend to skew any gross averages of the geosynchronous environment.

---

*The electron data for 1973, by which time these detectors had degraded, were corrected using a factor of 48 for the parallel detector and 0 for the detector perpendicular to the spin axis.

Table 1. Geomagnetic Activity for Days Analyzed

| Year | Day | Hourly AP | | | | | | | | Daily AP |
|---|---|---|---|---|---|---|---|---|---|---|
| 1972 | 217 | 67 | 236 | 132 | 27 | 56 | 27 | 111 | 400 | 1056 |
| 1970 | 348 | 22 | 80 | 236 | 48 | 32 | 15 | 32 | 56 | 521 |
| 1972 | 223 | 9 | 6 | 12 | 18 | 32 | 27 | 15 | 27 | 146 |
| 1969 | 326 | 15 | 18 | 12 | 7 | 5 | 5 | 12 | 6 | 80 |
| 1970 | 273 | 6 | 18 | 18 | 5 | 7 | 6 | 4 | 9 | 73 |
| 1970 | 272 | 3 | 5 | 6 | 5 | 2 | 3 | 2 | 12 | 38 |
| 1969 | 299 | 3 | 4 | 9 | 3 | 4 | 2 | 5 | 3 | 33 |
| 1970 | 25 | 4 | 3 | 2 | 0 | 2 | 2 | 3 | 4 | 20 |
| 1971 | 87 | 5 | 2 | 0 | 0 | 2 | 2 | 4 | 3 | 18 |
| 1970 | 345 | 0 | 2 | 3 | 3 | 2 | 0 | 2 | 2 | 14 |

As the purpose of this analysis is to model the time-history of a charging event, we have selected days exhibiting single injection events near satellite midnight, for the lower levels of geomagnetic activity. Such steps were based on the observation that spacecraft charging has been found to occur primarily in conjunction with individual plasma injections near midnight. This bias should be considered when evaluating the generality of the model.

## 5. RESULTS

A variety of parameters and combinations of parameters were calculated for this study. Considering the sparseness of the data base, we have limited the study to a formulation of the four moments in terms of linear regression-derived analytic expressions.* The currents and the parameters necessary for a Maxwellian and a 2 Maxwellian fit to the distribution function are computed from these predicted quantities. As a result of the simplicity of the fitted function (in particular the assumed linearity of $A_p$) and the paucity of data, some negative values result for the predicted values. As these, in turn, result in fictitious values for the derived quantities, in the FORTRAN formulation of the problem, these values have been corrected by estimates (see Table 2). With this caveat

*The average energy was calculated from the data and was derived from the fitted values. The latter values are used in this preliminary model to preserve the internal consistency of the model, since the differences between the values so derived are within the accuracy of the model.

Table 2. Default Values and Standard Deviations for Model

| Variable | Units | Electrons Std. Dev. /Default | | Ions Std. Dev. /Default | |
|---|---|---|---|---|---|
| Density | no#/cm$^3$ | 0.67 | 0.02 | 0.55 | 0.33 |
| Pressure | dynes/cm$^2$ | $2.6 \times 10^{-9}$ | $4 \times 10^{-11}$ | $4.9 \times 10^{-9}$ | $4 \times 19^{-9}$ |
| Energy flux | erg/(cm$^2$-sec-sr) | 2.1 | 0.08 | 0.13 | 0.09 |
| Number flux | no#/(cm$^2$ sec-sr) | $1.4 \times 10^8$ | $4 \times 10^6$ | $4 \times 10^6$ | $3 \times 10^6$ |
| Mean Energy | eV | (1600) | 1000 | (1820) | |
| Current | nAmps/cm$^2$ | 0.07 | 0.002 | 0.002 | 0.0015 |
| N1 | no#/cm$^3$ | | 2 | | |
| N2 | no#/cm$^3$ | | 0.04 | | |
| T1 | eV | | 250 | | |
| T2 | eV | | 20000 | | |

in mind, the model predictions will be discussed and, where possible, compared with other observations.

Tables 3 through 22 list, by parameter, the values predicted by the model (see FORTRAN listing in Appendices). The parameters are given as a function of the $A_p$ values corresponding to average daily values of $K_p$ of $0_o$, $1_o$, $2_o$, $3_o$, $4_o$, $5_o$, $6_o$, $7_o$, $8_o$, and $9_o$. As the data set of $A_p$ values includes only values as high as 1056 (that is, $K_p = 7_o$), the values for 1656 and 3200 should be treated as extrapolations. For each of the four moments and for the current, the standard deviation associated with the fit to the actual data is given. This is indicative of the error that should be assigned each predicted value. As would be expected for the small data set employed in this study, the predicted errors are a large fraction of the model values. Also, the environment actually exhibits large variations such as these.

In consideration of the errors associated with the four moments, it is not justified to draw more than a few generalized conclusions from the predictions of this preliminary model. In general, the ranges of the four moments well approximate those given by DeForest and McIlwain[5] in their Table 1 if their "maximum" values are taken as corresponding to an $A_p$ of ~ 1056 (average $K_p$ of $7_o$), their "typical" values as corresponding to $A_p$ of ~ 120 (average $K_p$ of $3_o$), and "minimum" to an $A_p$ of ~0 (average $K_p$ of $0_o$). The agreement is excellent for the ions as to actual

Table 3. Electron Density × 100 (number/$cm^3$)

| DAILY AP | LOCAL TIME 1.5 | 4.5 | 7.5 | 10.5 | 13.5 | 16.5 | 19.5 | 22.5 | AVERAGE |
|---|---|---|---|---|---|---|---|---|---|
| 3200 | 1418.7 | 1389.6 | 1697.1 | 1918.1 | 1434.4 | 892.9 | 1049.6 | 1449.2 | 1400.0 |
| 1656 | 782.8 | 738.6 | 895.7 | 1081.5 | 751.8 | 463.1 | 539.4 | 768.8 | 743.8 |
| 1056 | 534.6 | 585.0 | 585.5 | 645.2 | 486.5 | 295.1 | 341.1 | 584.3 | 487.7 |
| 640 | 367.1 | 363.1 | 373.4 | 398.3 | 302.6 | 189.3 | 203.6 | 321.0 | 310.7 |
| 384 | 257.5 | 243.6 | 241.8 | 246.3 | 189.5 | 103.1 | 119.0 | 208.2 | 201.8 |
| 216 | 188.2 | 178.1 | 154.1 | 146.5 | 115.7 | 62.3 | 63.5 | 134.1 | 130.3 |
| 128 | 144.2 | 140.7 | 106.5 | 89.5 | 72.7 | 35.6 | 31.8 | 91.8 | 89.4 |
| 56 | 122.3 | 115.8 | 71.4 | 51.6 | 44.4 | 17.8 | 10.6 | 63.6 | 62.2 |
| 32 | 112.4 | 106.4 | 59.0 | 32.3 | 33.5 | 11.1 | 2.7 | 53.0 | 52.0 |
| 0 | 99.2 | 94.0 | 42.6 | 18.3 | 19.7 | 2.2 | 2.0 | 38.9 | 39.6 |

Table 4. Ion Density × 100 (number/$cm^3$)

| DAILY AP | LOCAL TIME 1.5 | 4.5 | 7.5 | 10.5 | 13.5 | 16.5 | 19.5 | 22.5 | AVERAGE |
|---|---|---|---|---|---|---|---|---|---|
| 3200 | 644.1 | 537.0 | 831.0 | 1064.9 | 640.6 | 602.3 | 733.9 | 852.3 | 764.1 |
| 1656 | 390.4 | 338.0 | 490.0 | 601.3 | 477.0 | 345.9 | 414.5 | 486.7 | 443.0 |
| 1056 | 291.8 | 260.7 | 354.8 | 421.2 | 335.8 | 246.3 | 290.4 | 344.5 | 318.2 |
| 640 | 223.5 | 207.1 | 261.0 | 296.3 | 237.8 | 177.2 | 204.3 | 246.0 | 231.6 |
| 384 | 181.4 | 174.1 | 203.5 | 219.4 | 177.6 | 134.7 | 151.3 | 185.4 | 178.4 |
| 216 | 153.8 | 152.5 | 165.4 | 169.0 | 138.0 | 105.8 | 116.6 | 145.6 | 143.5 |
| 128 | 138.0 | 140.1 | 143.8 | 140.1 | 115.4 | 90.8 | 96.7 | 122.3 | 123.5 |
| 56 | 127.5 | 131.9 | 123.3 | 120.9 | 100.4 | 81.2 | 83.5 | 107.7 | 110.2 |
| 32 | 123.6 | 128.8 | 123.9 | 113.7 | 94.7 | 75.2 | 78.5 | 102.0 | 105.2 |
| 0 | 118.3 | 124.6 | 115.7 | 104.1 | 87.2 | 71.9 | 71.9 | 94.4 | 98.5 |

Table 5. Electron Pressure × $10^{10}$ (dynes/$cm^2$)

| DAILY AP | LOCAL TIME 1.5 | 4.5 | 7.5 | 10.5 | 13.5 | 16.5 | 19.5 | 22.5 | AVERAGE |
|---|---|---|---|---|---|---|---|---|---|
| 3200 | 600.2 | 423.8 | 515.2 | 585.8 | 474.1 | 282.7 | 242.8 | 340.3 | 408.1 |
| 1656 | 216.1 | 223.3 | 270.5 | 301.7 | 244.0 | 145.4 | 124.0 | 178.4 | 213.7 |
| 1056 | 144.6 | 154.0 | 175.5 | 191.3 | 154.6 | 92.1 | 72.9 | 115.2 | 130.1 |
| 640 | 95.0 | 101.8 | 103.5 | 114.8 | 92.7 | 55.1 | 45.6 | 71.4 | 85.8 |
| 384 | 64.5 | 69.7 | 63.0 | 67.7 | 54.5 | 32.3 | 26.1 | 44.5 | 53.5 |
| 216 | 44.5 | 68.6 | 42.4 | 36.6 | 29.5 | 17.4 | 13.2 | 26.8 | 32.4 |
| 128 | 33.1 | 35.6 | 27.1 | 19.1 | 15.2 | 8.8 | 5.8 | 16.7 | 20.3 |
| 56 | 25.4 | 28.5 | 17.0 | 7.3 | 5.6 | 3.2 | .9 | 10.0 | 12.2 |
| 32 | 22.6 | 25.5 | 13.2 | 2.9 | 2.1 | 1.0 | .4 | 7.4 | 9.4 |
| 0 | 18.5 | 21.5 | 5.1 | .4 | .4 | .4 | .4 | 4.1 | 6.8 |

Table 6. Ion Pressure $\times 10^{10}$ (dynes/cm$^2$)

| DAILY AP | LOCAL TIME 1.5 | 4.5 | 7.5 | 10.5 | 13.5 | 16.5 | 19.5 | 22.5 | AVERAGE |
|---|---|---|---|---|---|---|---|---|---|
| 3280 | 842.3 | 573.8 | 617.9 | 702.2 | 419.4 | 181.6 | 486.1 | 908.0 | 531.4 |
| 1656 | 482.2 | 335.5 | 353.3 | 393.1 | 247.8 | 127.4 | 289.1 | 513.5 | 343.1 |
| 1056 | 342.3 | 247.1 | 250.5 | 223.0 | 181.1 | 105.3 | 212.6 | 360.2 | 246.6 |
| 640 | 245.3 | 183.7 | 173.2 | 189.7 | 174.9 | 91.7 | 159.6 | 253.9 | 179.8 |
| 384 | 185.7 | 144.7 | 135.4 | 138.5 | 106.4 | 82.7 | 126.9 | 188.5 | 138.6 |
| 216 | 146.5 | 119.1 | 105.6 | 104.3 | 87.8 | 75.8 | 105.5 | 145.6 | 111.6 |
| 128 | 124.1 | 104.5 | 93.1 | 85.6 | 77.1 | 73.4 | 93.2 | 121.0 | 96.1 |
| 56 | 109.2 | 94.7 | 73.2 | 72.8 | 70.0 | 71.1 | 85.1 | 104.7 | 85.8 |
| 32 | 103.6 | 81.0 | 75.0 | 65.0 | 67.3 | 70.3 | 82.0 | 98.6 | 82.0 |
| 0 | 96.1 | 85.2 | 63.6 | 61.6 | 63.8 | 69.2 | 77.9 | 90.4 | 76.8 |

Table 7. Electron Energy Flux $\times$ 100 (erg/cm$^2$ sec-sr)

| DAILY AP | LOCAL TIME 1.5 | 4.5 | 7.5 | 10.5 | 13.5 | 16.5 | 19.5 | 22.5 | AVERAGE |
|---|---|---|---|---|---|---|---|---|---|
| 3280 | 2098.8 | 2351.2 | 3496.0 | 4895.3 | 4632.4 | 2820.5 | 1618.1 | 1770.2 | 2959.3 |
| 1656 | 1137.5 | 1286.2 | 1845.8 | 2524.8 | 2375.0 | 1447.7 | 836.6 | 936.2 | 1548.7 |
| 1056 | 767.8 | 872.3 | 1204.5 | 1603.6 | 1497.8 | 914.2 | 533.0 | 612.0 | 1000.6 |
| 640 | 510.2 | 585.4 | 753.8 | 964.9 | 889.6 | 544.4 | 322.4 | 387.3 | 620.5 |
| 384 | 352.1 | 408.8 | 486.2 | 571.8 | 515.3 | 313.8 | 192.9 | 249.0 | 386.6 |
| 216 | 248.4 | 292.9 | 305.7 | 318.9 | 269.6 | 167.4 | 107.8 | 158.3 | 233.1 |
| 128 | 189.1 | 226.2 | 204.1 | 166.5 | 129.3 | 82.0 | 59.2 | 106.4 | 145.4 |
| 56 | 149.6 | 182.6 | 135.5 | 68.3 | 35.7 | 25.1 | 26.9 | 71.8 | 87.0 |
| 32 | 134.8 | 166.0 | 113.0 | 31.4 | 8.0 | 3.0 | 14.7 | 58.9 | 66.5 |
| 0 | 115.0 | 144.0 | 75.8 | 8.0 | 8.0 | 3.0 | 8.0 | 41.6 | 51.0 |

Table 8. Ion Energy Flux $\times$ 100 (erg/cm$^2$ sec-sr)

| DAILY AP | LOCAL TIME 1.5 | 4.5 | 7.5 | 10.5 | 13.5 | 16.5 | 19.5 | 22.5 | AVERAGE |
|---|---|---|---|---|---|---|---|---|---|
| 3280 | 223.0 | 134.7 | 123.2 | 155.4 | 94.9 | 32.9 | 110.5 | 232.7 | 139.4 |
| 1656 | 126.0 | 80.4 | 75.1 | 87.9 | 56.9 | 25.5 | 66.5 | 130.7 | 81.1 |
| 1056 | 88.3 | 58.6 | 54.0 | 61.7 | 42.1 | 22.6 | 49.3 | 91.0 | 58.5 |
| 640 | 62.2 | 43.4 | 39.4 | 43.5 | 31.9 | 20.6 | 37.5 | 63.5 | 42.7 |
| 384 | 46.1 | 34.6 | 33.5 | 32.3 | 25.6 | 13.3 | 30.2 | 46.6 | 33.1 |
| 216 | 35.6 | 28.0 | 24.6 | 25.0 | 21.4 | 15.5 | 25.4 | 35.5 | 26.7 |
| 128 | 29.5 | 24.5 | 21.2 | 20.8 | 19.1 | 13.1 | 22.6 | 29.2 | 23.1 |
| 56 | 25.5 | 22.1 | 13.0 | 18.0 | 17.5 | 17.7 | 20.8 | 25.0 | 20.7 |
| 32 | 24.0 | 21.2 | 18.1 | 16.9 | 16.9 | 17.6 | 20.1 | 23.4 | 19.8 |
| 0 | 22.0 | 20.1 | 17.8 | 15.5 | 16.1 | 17.5 | 19.2 | 21.3 | 18.6 |

Table 9. Electron Number Flux $\times 10^{-6}$ (number/$cm^2$ sec-sr)

| DAILY AP | LOCAL TIME 1.5 | 4.5 | 7.5 | 10.5 | 13.5 | 16.5 | 19.5 | 22.5 | AVERAGE |
|---|---|---|---|---|---|---|---|---|---|
| 3200 | 3841.1 | 3076.6 | 3355.7 | 3313.3 | 2375.9 | 1434.7 | 1784.0 | 2672.3 | 2639.2 |
| 1656 | 1645.5 | 1665.0 | 1761.8 | 1714.3 | 1236.7 | 773.8 | 910.3 | 1401.2 | 1388.5 |
| 1056 | 1101.1 | 1116.5 | 1142.4 | 1092.6 | 794.0 | 493.6 | 570.7 | 907.3 | 902.5 |
| 640 | 727.1 | 736.2 | 712.9 | 662.0 | 457.0 | 293.4 | 335.3 | 564.8 | 565.6 |
| 384 | 495.7 | 502.1 | 448.6 | 396.9 | 298.1 | 173.9 | 198.5 | 354.0 | 358.2 |
| 216 | 343.5 | 348.6 | 275.2 | 222.9 | 174.2 | 101.4 | 95.4 | 215.7 | 222.1 |
| 120 | 257.1 | 260.8 | 176.1 | 123.5 | 103.3 | 55.6 | 41.1 | 136.7 | 144.4 |
| 56 | 199.2 | 202.3 | 110.0 | 57.2 | 56.1 | 25.7 | 4.9 | 84.0 | 92.5 |
| 32 | 177.5 | 180.4 | 85.3 | 32.3 | 38.4 | 15.5 | 4.0 | 64.2 | 74.7 |
| 0 | 146.6 | 151.1 | 52.2 | 4.0 | 14.8 | 4.0 | 4.0 | 37.9 | 52.1 |

Table 10. Ion Number Flux $\times 10^{-6}$ (number/$cm^2$ sec-sr)

| DAILY AP | LOCAL TIME 1.5 | 4.5 | 7.5 | 10.5 | 13.5 | 16.5 | 19.5 | 22.5 | AVERAGE |
|---|---|---|---|---|---|---|---|---|---|
| 1280 | 63.7 | 48.4 | 68.8 | 70.0 | 45.3 | 24.1 | 46.4 | 71.3 | 53.5 |
| 1656 | 36.3 | 25.9 | 34.4 | 38.6 | 25.8 | 14.9 | 25.8 | 40.4 | 30.7 |
| 1656 | 26.5 | 21.1 | 24.1 | 26.5 | 18.2 | 11.3 | 18.5 | 28.4 | 21.8 |
| 648 | 19.3 | 15.8 | 17.0 | 19.0 | 12.9 | 8.8 | 13.5 | 20.1 | 15.7 |
| 384 | 14.9 | 12.5 | 12.6 | 12.4 | 9.7 | 7.3 | 10.4 | 15.0 | 11.9 |
| 216 | 12.0 | 10.3 | 8.7 | 9.4 | 7.6 | 6.3 | 8.4 | 11.6 | 9.6 |
| 120 | 10.3 | 9.1 | 8.1 | 7.5 | 6.4 | 5.7 | 7.2 | 9.7 | 8.0 |
| 55 | 9.2 | 8.3 | 7.0 | 6.2 | 5.6 | 5.3 | 6.5 | 8.4 | 7.1 |
| 32 | 8.8 | 8.0 | 6.6 | 5.2 | 5.3 | 5.2 | 6.2 | 8.0 | 6.7 |
| 0 | 8.3 | 7.8 | 6.0 | 5.1 | 4.9 | 5.0 | 5.8 | 7.3 | 6.2 |

Table 11. Electron Mean Energy (eV)

| DAILY AP | LOCAL TIME 1.5 | 4.5 | 7.5 | 10.5 | 13.5 | 16.5 | 19.5 | 22.5 | AVERAGE |
|---|---|---|---|---|---|---|---|---|---|
| 3280 | 2640.2 | 2955.4 | 2841.4 | 2858.4 | 3093.8 | 2963.3 | 2165.3 | 2201.7 | 2714.9 |
| 1556 | 2587.8 | 2385.4 | 2817.4 | 2819.7 | 3038.4 | 2933.7 | 2152.1 | 2171.6 | 2678.8 |
| 1856 | 2532.2 | 2854.8 | 2793.6 | 2775.1 | 2975.0 | 2903.6 | 2136.3 | 2138.4 | 2638.9 |
| 640 | 2450.5 | 2777.1 | 2745.9 | 2697.4 | 2865.7 | 2853.5 | 2107.3 | 2082.9 | 2573.1 |
| 384 | 2345.6 | 2670.1 | 2678.7 | 2572.0 | 2692.8 | 2772.7 | 2056.2 | 2000.3 | 2474.7 |
| 216 | 2213.2 | 2555.1 | 2571.8 | 2348.4 | 2395.1 | 2603.7 | 1948.5 | 1870.4 | 2314.0 |
| 124 | 2082.1 | 2432.5 | 2431.8 | 1996.9 | 1951.8 | 2324.5 | 1718.2 | 1702.2 | 2079.9 |
| 56 | 1947.6 | 2306.8 | 2225.4 | 1330.9 | 1185.9 | 1659.4 | 1000.0 | 1465.8 | 1640.5 |
| 32 | 1858.4 | 2244.4 | 2893.7 | 731.4 | 1000.0 | 1000.0 | 1000.0 | 1312.3 | 1407.8 |
| 0 | 1771.1 | 2145.1 | 1791.8 | 1000.0 | 1000.0 | 1000.0 | 1000.0 | 977.8 | 1335.4 |

Table 12. Ion Mean Energy (eV)

| DAILY AP | LOCAL TIME 1.5 | 4.5 | 7.5 | 10.5 | 13.5 | 16.5 | 19.5 | 22.5 | AVERAGE |
|---|---|---|---|---|---|---|---|---|---|
| 3280 | 12240.5 | 10801.9 | 6901.1 | 6172.0 | 4670.5 | 2827.2 | 6198.9 | 9971.0 | 7372.3 |
| 1656 | 11562.3 | 9373.7 | 6743.0 | 6118.9 | 4652.3 | 3445.7 | 6529.2 | 9876.2 | 7314.8 |
| 1056 | 10983.5 | 8870.0 | 6609.4 | 6066.8 | 5048.9 | 4040.2 | 6853.7 | 9785.0 | 7281.9 |
| 640 | 10276.3 | 8301.9 | 6427.6 | 5993.4 | 5308.3 | 4843.5 | 7310.1 | 9660.0 | 7265.1 |
| 384 | 9578.5 | 7777.6 | 6232.5 | 5906.4 | 5610.2 | 5747.3 | 7849.1 | 9517.1 | 7277.4 |
| 216 | 8913.5 | 7310.2 | 6030.4 | 5807.1 | 5951.5 | 6731.6 | 8468.9 | 9358.5 | 7321.5 |
| 120 | 8414.2 | 6978.4 | 5867.1 | 5717.8 | 6251.6 | 7565.4 | 9023.1 | 9221.8 | 7379.9 |
| 56 | 8012.7 | 6722.6 | 5727.9 | 5634.7 | 6526.7 | 8305.3 | 9539.0 | 9098.6 | 7446.0 |
| 32 | 7944.5 | 6618.2 | 5667.4 | 5596.3 | 6652.5 | 8636.0 | 9777.4 | 9043.0 | 7479.4 |
| 0 | 7602.8 | 6470.9 | 5577.9 | 5536.9 | 6845.5 | 9134.7 | 10146.4 | 8958.4 | 7534.2 |

Table 13. Electron Current $\times 10^4$ (n amps/cm$^2$)

| DAILY AP | LOCAL TIME 1.5 | 4.5 | 7.5 | 10.5 | 13.5 | 16.5 | 19.5 | 22.5 | AVERAGE |
|---|---|---|---|---|---|---|---|---|---|
| 3280 | 15286.4 | 15463.9 | 16867.7 | 16654.6 | 11942.7 | 7513.1 | 8967.2 | 13432.4 | 13266.0 |
| 1656 | 8271.1 | 8369.1 | 8855.7 | 8616.8 | 6216.2 | 3883.4 | 4575.4 | 7043.2 | 6979.6 |
| 1056 | 5545.9 | 5612.0 | 5742.2 | 5493.2 | 3990.9 | 2481.3 | 2868.8 | 4560.3 | 4536.7 |
| 640 | 3654.8 | 3700.4 | 3583.5 | 3327.6 | 2448.0 | 1504.9 | 1685.5 | 2038.9 | 2843.0 |
| 384 | 2491.7 | 2524.1 | 2265.1 | 1984.3 | 1498.5 | 904.1 | 957.3 | 1779.5 | 1800.7 |
| 216 | 1728.3 | 1752.1 | 1383.4 | 1120.3 | 875.4 | 509.8 | 479.5 | 1084.3 | 1116.6 |
| 120 | 1292.2 | 1311.8 | 885.2 | 620.6 | 519.3 | 284.5 | 206.4 | 687.1 | 725.8 |
| 56 | 1001.4 | 1016.9 | 553.1 | 287.4 | 282.8 | 134.3 | 24.4 | 422.2 | 465.2 |
| 32 | 892.3 | 906.6 | 428.6 | 162.5 | 193.0 | 73.0 | 20.1 | 322.9 | 375.5 |
| 0 | 746.3 | 759.5 | 262.5 | 20.1 | 74.3 | 20.1 | 20.1 | 190.5 | 261.8 |

Table 14. Ion Current $\times 10^4$ (n amps/cm$^2$)

| DAILY AP | LOCAL TIME 1.5 | 4.5 | 7.5 | 10.5 | 13.5 | 15.5 | 19.5 | 22.5 | AVERAGE |
|---|---|---|---|---|---|---|---|---|---|
| 3280 | 320.0 | 245.1 | 305.8 | 351.6 | 227.5 | 121.. | 223.0 | 358.5 | 269.1 |
| 1656 | 185.7 | 145.1 | 172.8 | 194.2 | 129.5 | 76.8 | 129.5 | 203.3 | 154.4 |
| 1056 | 153.4 | 106.3 | 121.1 | 133.1 | 91.4 | 55.8 | 93.1 | 143.0 | 109.8 |
| 640 | 97.2 | 79.4 | 85.3 | 90.7 | 65.0 | 44.3 | 67.9 | 101.2 | 78.9 |
| 384 | 75.0 | 62.8 | 63.3 | 64.6 | 48.8 | 35.6 | 52.4 | 75.4 | 59.9 |
| 216 | 60.3 | 52.0 | 49.8 | 47.4 | 38.1 | 31.6 | 42.2 | 58.5 | 47.4 |
| 120 | 52.0 | 45.2 | 48.5 | 37.7 | 32.8 | 28.7 | 36.4 | 48.9 | 40.2 |
| 56 | 46.4 | 41.6 | 35.0 | 31.1 | 27.9 | 26.8 | 32.5 | 42.5 | 35.5 |
| 32 | 44.3 | 40.0 | 33.8 | 28.7 | 26.4 | 25.0 | 31.1 | 40.0 | 33.7 |
| 0 | 41.6 | 38.0 | 33.2 | 25.4 | 24.4 | 25.1 | 29.2 | 36.8 | 31.8 |

Table 15. Electron Density 1 × 100 (number/$cm^3$)

| DAILY AP | 1.5 | 4.5 | 7.5 | 10.5 | 13.5 | 16.5 | 19.5 | 22.5 | AVERAGE |
|---|---|---|---|---|---|---|---|---|---|
| | LOCAL TIME | | | | | | | | |
| 3200 | 1247.5 | 1310.9 | 1228.5 | 1477.1 | 1158.2 | 753.0 | 888.4 | 878.5 | 1118.4 |
| 1556 | 653.9 | 701.6 | 655.0 | 776.5 | 610.2 | 394.2 | 460.2 | 491.2 | 532.9 |
| 1056 | 421.8 | 459.2 | 432.1 | 504.2 | 392.2 | 252.9 | 293.6 | 338.9 | 388.3 |
| 640 | 278.3 | 298.0 | 277.5 | 315.4 | 249.6 | 154.9 | 177.8 | 230.6 | 246.8 |
| 384 | 192.6 | 181.0 | 182.4 | 199.2 | 156.6 | 84.6 | 106.0 | 161.0 | 160.7 |
| 216 | 140.1 | 133.2 | 113.9 | 122.6 | 99.3 | 55.0 | 58.2 | 111.9 | 105.2 |
| 128 | 113.5 | 104.2 | 84.0 | 78.9 | 65.3 | 32.5 | 30.2 | 81.4 | 73.8 |
| 56 | 96.9 | 85.7 | 53.9 | 49.0 | 42.9 | 17.4 | 10.6 | 59.3 | 52.7 |
| 32 | 89.6 | [illegible] | 63.4 | 37.0 | 33.6 | 11.1 | 2.7 | 50.5 | 44.5 |
| 0 | 81.1 | 77.5 | 35.3 | 18.3 | 19.7 | 2.2 | 2.0 | 38.2 | 34.0 |

Table 16. Ion Density 1 × 100 (number/$cm^3$)

| DAILY AP | 1.5 | 4.5 | 7.5 | 10.5 | 13.5 | 16.5 | 19.5 | 22.5 | AVERAGE |
|---|---|---|---|---|---|---|---|---|---|
| | LOCAL TIME | | | | | | | | |
| 3200 | 162.2 | 151.8 | 234.5 | 675.6 | 629.5 | 424.0 | 378.8 | 325.2 | 371.0 |
| 1556 | 121.3 | 112.1 | 193.3 | 329.3 | 328.4 | 236.6 | 206.3 | 183.6 | 214.6 |
| 1056 | 95.6 | [illegible] | 154.3 | 232.7 | 224.1 | 161.8 | 139.4 | 128.5 | 153.8 |
| 640 | 77.5 | 82.3 | 122.9 | 166.5 | 152.8 | 103.3 | 93.1 | 90.3 | 111.8 |
| 384 | 66.2 | 75.0 | 108.3 | 126.2 | 109.9 | 75.9 | 64.8 | 66.8 | 86.1 |
| 216 | 58.5 | 70.2 | 93.2 | 100.1 | 82.4 | 55.9 | 46.3 | 51.3 | 69.4 |
| 128 | 53.3 | 67.6 | 82.5 | 85.3 | 67.1 | 44.0 | 35.9 | 42.5 | 59.8 |
| 56 | 50.5 | 65.7 | 77.4 | 75.5 | 57.1 | 35.2 | 29.0 | 36.6 | 53.5 |
| 32 | 48.4 | 65.0 | 75.4 | 71.9 | 53.4 | 33.3 | 26.4 | 34.4 | 51.1 |
| 0 | 47.7 | 64.1 | 72.7 | 67.0 | 48.6 | 23.5 | 23.0 | 31.4 | 48.0 |

Table 17. Electron Temperature 1 (eV)

| DAILY AP | 1.5 | 4.5 | 7.5 | 10.5 | 13.5 | 16.5 | 19.5 | 22.5 | AVERAGE |
|---|---|---|---|---|---|---|---|---|---|
| | LOCAL TIME | | | | | | | | |
| 3200 | 1243.1 | 1725.4 | 631.9 | 270.3 | 222.6 | 323.5 | 533.9 | 455.8 | 669.1 |
| 1556 | 1142.1 | 1562.2 | 520.4 | 270.6 | 227.8 | 334.7 | 531.6 | 469.8 | 632.4 |
| 1056 | 1015.7 | 1335.4 | 507.0 | 271.0 | 233.0 | 340.9 | 528.2 | 481.4 | 595.7 |
| 640 | 862.7 | 1140.6 | 488.2 | 271.4 | 244.6 | 351.9 | 520.6 | 493.2 | 546.6 |
| 384 | 717.3 | 888.8 | 469.4 | 271.9 | 261.9 | 373.8 | 503.5 | 497.7 | 496.6 |
| 216 | 587.4 | 666.6 | 420.9 | 271.9 | 292.7 | 405.0 | 459.7 | 485.0 | 448.9 |
| 128 | 495.5 | 517.2 | 374.1 | 269.5 | 341.2 | 477.1 | 354.2 | 449.9 | 410.1 |
| 56 | 424.3 | 413.4 | 316.2 | 254.1 | 431.5 | 645.3 | 250.0 | 386.3 | 390.1 |
| 32 | 395.0 | 372.3 | 282.1 | 219.5 | 250.0 | 250.0 | 250.0 | 342.2 | 295.1 |
| 0 | 353.8 | 316.2 | 215.0 | 250.0 | 250.0 | 250.0 | 250.0 | 247.3 | 266.4 |

Table 18. Ion Temperature 1 (eV)

| DAILY AP | LOCAL TIME 1.5 | 4.5 | 7.5 | 10.5 | 13.5 | 16.5 | 19.5 | 22.5 | AVERAGE |
|---|---|---|---|---|---|---|---|---|---|
| 3280 | 158.3 | 267.6 | 187.4 | 379.8 | 434.5 | 175.6 | 61.0 | 73.2 | 216.6 |
| 1656 | 113.7 | 168.5 | 155.5 | 305.9 | 346.2 | 143.3 | 44.0 | 57.3 | 166.9 |
| 1056 | 89.8 | 121.4 | 133.0 | 248.2 | 270.1 | 108.9 | 29.6 | 43.8 | 130.6 |
| 640 | 64.3 | 87.3 | 113.1 | 184.6 | 184.3 | 65.7 | 13.7 | 28.1 | 92.8 |
| 384 | 45.6 | 65.8 | 89.6 | 129.2 | 109.4 | 27.6 | 2.4 | 14.3 | 60.5 |
| 216 | 30.4 | 51.9 | 72.2 | 83.8 | 51.5 | 3.7 | 1.1 | 4.3 | 37.4 |
| 120 | 28.7 | 44.2 | 68.3 | 55.0 | 20.1 | 1.2 | 12.1 | .3 | 26.7 |
| 56 | 13.9 | 39.2 | 51.4 | 35.5 | 4.6 | 15.2 | 34.5 | .6 | 24.4 |
| 32 | 11.4 | 37.7 | 47.8 | 28.4 | 1.2 | 27.1 | 49.3 | 2.8 | 25.6 |
| 0 | 8.0 | 34.9 | 42.6 | 19.4 | .2 | 52.2 | 78.3 | 5.6 | 30.2 |

Table 19. Electron Density 2 × 100 (number/cm$^3$)

| DAILY AP | LOCAL TIME 1.5 | 4.5 | 7.5 | 10.5 | 13.5 | 16.5 | 19.5 | 22.5 | AVERAGE |
|---|---|---|---|---|---|---|---|---|---|
| 3280 | 171.2 | 24.7 | 468.5 | 441.[illegible] | 226.2 | 134.9 | 161.2 | 570.7 | 281.6 |
| 1656 | 128.2 | 37.0 | 243.8 | 225.0 | 141.6 | 68.9 | 79.2 | 277.5 | 158.1 |
| 1056 | 106.6 | 45.9 | 156.4 | 141.0 | 89.3 | 43.3 | 47.5 | 165.5 | 99.4 |
| 640 | 84.5 | 53.2 | 95.8 | 82.6 | 57.0 | 25.5 | 25.9 | 90.4 | 63.9 |
| 384 | 64.9 | 62.6 | 58.6 | 47.1 | 30.7 | 14.5 | 13.0 | 47.2 | 41.1 |
| 216 | 47.3 | 44.8 | 34.2 | 23.8 | 15.9 | 7.3 | 5.3 | 22.2 | 25.1 |
| 120 | 35.2 | 36.5 | 22.5 | 10.7 | 7.4 | 3.1 | 1.6 | 10.4 | 15.7 |
| 56 | 26.3 | 29.1 | 11.5 | 2.6 | 1.6 | .4 | .2 | 4.3 | 9.5 |
| 32 | 22.8 | 25.9 | 8.2 | .3 | .7 | .2 | .1 | 2.5 | 7.6 |
| 0 | 18.1 | 21.5 | 4.1 | .4 | .4 | .0 | .0 | .8 | 5.7 |

Table 20. Ion Density 2 × 100 (number/cm$^3$)

| DAILY AP | LOCAL TIME 1.5 | 4.5 | 7.5 | 10.5 | 13.5 | 15.5 | 19.5 | 22.5 | AVERAGE |
|---|---|---|---|---|---|---|---|---|---|
| 3280 | 456.8 | 378.2 | 523.5 | 485.1 | 241.8 | 173.3 | 355.1 | 527.1 | 393.1 |
| 1656 | 269.1 | 225.9 | 293.7 | 272.0 | 148.7 | 103.3 | 208.1 | 303.1 | 228.4 |
| 1056 | 196.2 | 166.3 | 201.5 | 188.4 | 111.7 | 84.5 | 150.9 | 216.1 | 164.3 |
| 640 | 145.3 | 124.8 | 138.1 | 123.6 | 85.0 | 67.9 | 111.2 | 155.7 | 119.8 |
| 384 | 115.2 | 99.2 | 108.8 | 93.2 | 67.7 | 57.7 | 86.6 | 118.6 | 92.3 |
| 216 | 95.3 | 82.3 | 75.2 | 68.9 | 55.6 | 50.9 | 70.3 | 94.3 | 74.1 |
| 120 | 84.2 | 72.6 | 61.2 | 54.8 | 48.3 | 45.9 | 60.9 | 80.4 | 63.7 |
| 56 | 76.3 | 66.2 | 52.8 | 45.4 | 43.2 | 44.0 | 54.5 | 71.1 | 56.7 |
| 32 | 74.2 | 63.7 | 48.6 | 41.0 | 41.3 | 42.9 | 52.1 | 67.6 | 54.0 |
| 0 | 70.7 | 60.5 | 54.0 | 37.1 | 38.6 | 41.4 | 48.9 | 63.0 | 58.5 |

Table 21. Electron Temperature 2 (eV)

| DAILY AP | LOCAL TIME 1.5 | 4.5 | 7.5 | 10.5 | 13.5 | 16.5 | 19.5 | 22.5 | AVERAGE |
|---|---|---|---|---|---|---|---|---|---|
| 3200 | 5251.3 | 13257.8 | 5473.9 | 7390.8 | 97[illegible].3 | 11237.9 | 6467.3 | 3029.6 | 7737.6 |
| 1556 | 4708.4 | 9082.5 | 5534.7 | 7443.4 | 9764.6 | 11266.5 | 6696.2 | 3183.4 | 7212.5 |
| 1056 | 4397.4 | 7095.7 | 5604.7 | 7506.5 | 9777.3 | 11301.7 | 6973.3 | 3363.0 | 7002.4 |
| 640 | 4169.7 | 5742.0 | 5725.8 | 7622.4 | 9765.8 | 11363.2 | 7492.0 | 3678.9 | 6945.7 |
| 384 | 4081.3 | 5060.2 | 5918.4 | 7827.5 | 9751.0 | 11497.1 | 8438.8 | 4189.9 | 7095.6 |
| 216 | 4127.3 | 4790.5 | 6252.5 | 8261.3 | 9738.5 | 116[illegible].7 | 10582.2 | 5095.7 | 7581.5 |
| 128 | 4271.7 | 4779.6 | 6751.3 | 9197.9 | 9773.7 | 126[illegible].3 | 16121.0 | 6500.4 | 8754.4 |
| 56 | 4494.7 | 4899.5 | 7610.8 | 12990.1 | 10490.5 | 19595.3 | 20000.0 | 9135.7 | 11152.5 |
| 32 | 4631.5 | 4932.7 | 8298.1 | 29003.7 | 20000.0 | 20000.0 | 20000.0 | 11510.5 | 14804.6 |

Table 22. Ion Temperature 2 (eV)

| DAILY AP | LOCAL TIME 1.5 | 4.5 | 7.5 | 10.5 | 13.5 | 16.5 | 19.5 | 22.5 | AVERAGE |
|---|---|---|---|---|---|---|---|---|---|
| 3200 | 11456.1 | 9365.6 | 726[illegible].2 | 8589.4 | 9781.0 | 5945.1 | 8486.1 | 10715.2 | 8949.8 |
| 1656 | 11145.4 | 9276.1 | 7484.5 | 8657.0 | 9648.4 | 6958.0 | 8634.1 | 10548.2 | 9045.2 |
| 1056 | 10854.3 | 9210.5 | 7703.6 | 8743.8 | 9586.5 | 7649.3 | 8771.5 | 10398.1 | 9113.5 |
| 640 | 10467.3 | 9136.6 | 8008.6 | 8893.6 | 9577.1 | 8329.2 | 8953.7 | 10169.4 | 9191.9 |
| 384 | 10035.1 | 9065.6 | 8363.3 | 9105.0 | 9642.4 | 8909.3 | 9155.9 | 9920.2 | 9275.0 |
| 216 | 9573.4 | 8937.6 | 8763.5 | 9387.1 | 9780.7 | 9417.1 | 9375.4 | 9545.0 | 9368.1 |
| 120 | 9133.3 | 8945.7 | 9114.2 | 9671.4 | 9939.5 | 9787.0 | 9562.9 | 9408.6 | 9453.1 |
| 56 | 8850.1 | 8903.1 | 9434.5 | 9961.8 | 10106.2 | 10085.4 | 9732.2 | 9196.1 | 9534.9 |
| 32 | 8711.3 | 8884.9 | 9580.6 | 10104.3 | 10187.6 | 10212.0 | 9809.0 | 9110.4 | 9573.8 |
| 0 | 8430.1 | 8858.5 | 9804.2 | 10335.4 | 10317.4 | 10396.8 | 9926.7 | 8955.0 | 9635.5 |

amplitude and local time. The agreement is also quite good for the energy flux and number flux for the electrons, but not as good with the density and pressure (the model predicts two peaks – one near midnight and the other near 0930 in contrast to their single peak near midnight). In consideration of the greater variability of the electrons, this discrepancy is probably a real deviation.

Although skewed somewhat by the problems discussed in earlier sections of the paper (that is, injections and a less then random selection of events), the amplitudes of the four moments predicted by the model for the electrons and ions demonstrate consistent local time variations. For example, all show a sharp minimum between 1630 to 1930 local time for moderate to high levels of geomagnetic activity – the minima being on the order of 50 percent of the maximum values. At low values of geomagnetic activity and for the derived quantities, this trend is lost or greatly reduced. The minimum is obvious in most spectrograms returned by ATS-5 and ATS-6 and probably reflects the sharp edge of the plasma sheet/injection boundary in the evening hours reported by many others[11, 12, 13] which marks the boundary between eastward drifting low energy ions and westward drifting high energy ions.

In contrast to the minima, the peaks at high geomagnetic activity appear broad in extent and well-defined. At low levels of $A_p$, all moments peak between 0130 and 0430. The mean energies for the electrons are about one-fourth of expected values and show no strong local time or $A_p$ variation, although there may be a slight tendency for higher energies to occur, on the average near 0430 local time. The mean ion energies, in comparison, peak near midnight moving to earlier hours (~2000) as the geomagnetic activity decreases. Again, this would be consistent with the movement of the hot plasma sheet/injection boundary toward the evening hours at geosynchronous orbit during geomagnetic activity.

The derived quantities (mean energy, $N_1$, $N_2$, $T_1$, and $T_2$), although contaminated by minimum value estimates below $A_p$ ~ 56, reveal several features. As just described, the electron mean energy shows no strong variation with local time or $A_p$. This is consistent with the observations of ATS-5 data reported by

11. Vasyliunas, V.M. (1968) A survey of low energy electrons in the evening sector of the magnetosphere with Ogo 1 and Ogo 3, J. Geophys. Res., 73:2839.

12. McIlwain, C.E. (1971) Plasma convection in the vicinity of the geosynchronous orbit, Earth Magnetospheric Processes, B.M. McCormac, Ed., D. Reidel Publishing Co., Dordrecht, Holland.

13. Mauk, B., and McIlwain, C.E. (1974) Correlation of $K_p$ with the substorm-injected plasma boundary, J. Geophys. Res. 79:3193.

Inouye.[14] The estimates of the standard deviations of these values are on the order of ~1500 eV for the electrons and ~2000 eV for the ions, quantities of similar magnitude for the electrons as the change in the predicted values. This trend is evident in the 2 Maxwellian fits except, interestingly, the high energy temperature component of the electrons and ions. For them a trend toward higher values for the daily average temperature at lower levels of geomagnetic activity is significant and and in contrast to the increase in the daily average of all other parameters. This would lend support to the assumption of Inouye[14] and Stevens et al[7] that the plasma temperature goes up as the current goes down. The results imply, however, that the effect is dependent on how one defines the energy or temperature. The mean energy as defined in this study is ~1/4 of its expected value and usually increases. In fact, the temperature as represented by $T_2$ for the electrons and ions, not the mean energy, better represents the maximum values estimated by other studies.[7,4,15] Also, the maximum temperature and mean energy for the electrons are a factor 2 higher if maximum instead of average values are used in the study.

On the assumption that the 2 Maxwellian fit is a reasonable approximation to the actual plasma distribution, further observations can be made based on the model: First, it is the low temperature component ($T_1$) of the ions and electrons which shows the largest percentage increase as geomagnetic activity increases. Related to this is the observation that although the densities $N_1$ and $N_2$ increase markedly with geomagnetic activity, the ratio, $N_2/N_1$ of the daily averages of the densities remain roughly equal in spite of large local time variations in the ratios. This may indicate that the percentage of particles, as represented by their ratio $N_2/N_1$, in the two populations changes little on a daily basis, whereas their temperatures $T_1$ and $T_2$ are varying independent of each other (in fact, the high temperature components may be decreasing with geomagnetic activity). In consideration of the paucity of data in the analysis, however, these conclusions are tentative.

## 6. MODEL USAGE

In this section, two examples of model usage in estimating the effects of charging will be given. The model will be employed in estimating the environment

14. Inouye, G. T. (1976) Spacecraft potentials in a substorm environment, AIAA Progress in Astronautics and Aeronautics Series, Vol. 42, pp. 103-120.

15. DeForest, S. E. (1977) Final Report for 1 June 1976–30 November 1976, AFGL-TR-77-0031.

conducive to charging at geosynchronous orbit.* This environment can, in turn, be joined with a spacecraft charging model to give satellite potentials.

Of general interest is the prediction of the charging environment a satellite is likely to encounter during a typical mission. The basic idea is to predict the expected occurrence frequency of $A_p$ during the mission. This has been done for a "typical" time period in Figure 3 where a histogram of over 30 years of $A_p$ values has been plotted. The results of this figure can be utilized in two ways. First, the probability of observing a given interval of $A_p$ or, equivalently, a given level of geomagnetic activity can be found; for example, the probability of observing the $A_p$ interval 56-120 is 33 percent in a given time period. Similarly, the probability that a value of $A_p$ of 120 will be exceeded during a mission is given by:

$$P = 100\% - 14\%(A_p \le 32) - 23\%(32 < A_p \le 56) - 33\%(56 < A_p \le 120) = 30\% \quad .$$

The value of $A_p$ (120 in this example) can then be substituted into the model (see Appendices for a FORTRAN listing of the model) along with a local time between 0000 and 2400 to give the ambient environment expected 33 percent of the time, or not to be "exceeded" more than 30 percent of the time.

Substituting the $A_p$ value of 120 and a LT of 0130, the FORTRAN subroutine returns,* one notes:

| | Electron Population | Ion Population |
|---|---|---|
| Number density (no#/cm$^3$) | 1.49 | 1.38 |
| Pressure (dynes/cm$^2$) | $3.31 \times 10^{-9}$ | $1.24 \times 10^{-8}$ |
| Energy flux (erg/cm$^2$ sec-sr) | 1.89 | 0.30 |
| Number flux (no#/cm$^2$ sec-sr) | $2.57 \times 10^8$ | $10^7$ |
| Mean energy 3/2 kT (eV) | 2100 | 8400 |
| Current (amps/cm$^2$) | 0.13 | 0.005 |

*The model is not intended to be used to give total average plasma "dosages" since plasma injections occurring when the satellite was near local midnight were preferentially selected. Rather, it is intended to give the environment most conducive to charging – that is, following injections when the satellite is near local midnight.

*Note: These values are in very good agreement with DeForest and McIlwain[5] and Garrett et al[4] for "typical" values if 3/2 ($T_2$) is the "mean energy."

| | Electron Population | Ion Population |
|---|---|---|
| 2 Maxwellian: | | |
| N1 (no#/cm$^3$) | 1.13 | 0.54 |
| T1 (eV) | 496 | 21 |
| N2 (no#/cm$^3$) | 0.35 | 0.84 |
| T2 (eV) | 4270 | 9200 |

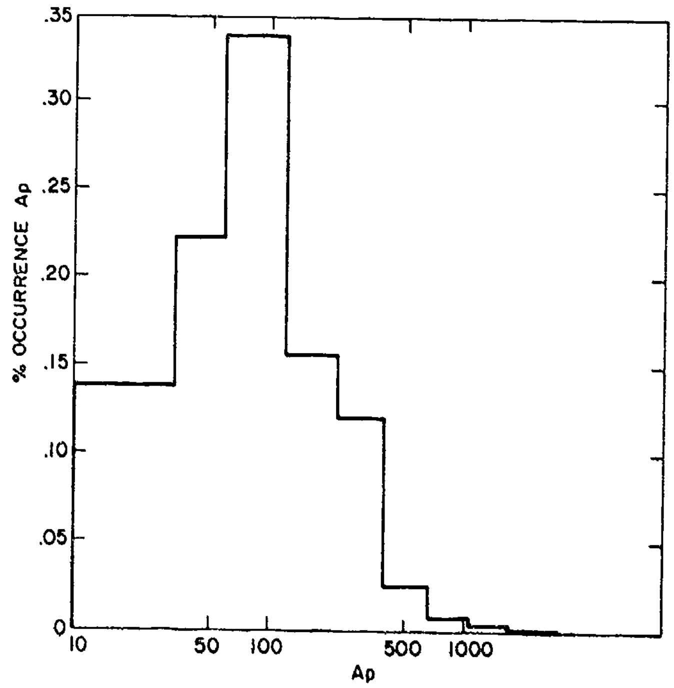


Figure 3. Histogram of the Occurrence Frequency of $A_p$, the Daily Sum of $a_p$, for the Years 1932 through 1975

The approximate distribution function (or particle spectrum) can then be derived by either of the following:

Electrons

$$f_e(E) = 27.2\ N_e \left(\frac{T_e}{1000}\right)^{-3/2} e^{-E/T_e} \tag{12a}$$

Ions

$$f_I(E) = 2.14 \times 10^6 \, N_I \left(\frac{T_I}{1000}\right)^{-3/2} e^{-E/T_I} \tag{12b}$$

where

$f_e, f_I$ = distribution functions ($sec^3 \, km^{-6}$)

$N_e$ = 1.49 $cm^{-3}$

$N_I$ = 1.38 $cm^{-3}$

$T_e$ = 2/3 (2100 eV) = 1400 eV

$T_I$ = 2/3 (8400 eV) = 5600 eV

E = particle energy (eV)

or:

$$f'_e(E) = 27.2 \left( N1_e \left(\frac{T1_e}{1000}\right)^{-3/2} e^{-E/T1_e} + N2_e \left(\frac{T2_e}{1000}\right)^{-3/2} e^{-E/T2_e} \right) \tag{13a}$$

$$f'_I(E) = 2.14 \times 10^6 \left( N1_I \left(\frac{T1_I}{1000}\right)^{-3/2} e^{-E/T1_I} + N2_I \left(\frac{T2_I}{1000}\right)^{-3/2} e^{-E/T2_I} \right) \tag{13b}$$

where

$f'_e, f'_I$ = distribution functions ($sec^3 \, km^{-6}$)

| | |
|---|---|
| $N1_e$ = 1.13 $cm^{-3}$ | $N1_I$ = 0.54 $cm^{-3}$ |
| $T1_e$ = 496 eV | $T1_I$ = 21 eV |
| $N2_e$ = 0.35 $cm^{-3}$ | $N2_I$ = 0.84 $cm^{-3}$ |
| $T2_e$ = 4270 eV | $T2_I$ = 9200 eV |

The resulting distribution functions are plotted in Figures 4 and 5. It is recommended that Eq. (13) be used for $A_p$ greater than 50, and Eq. (12) for lower values.

A second use of the model is in making real time estimates of the plasma conditions. A provisional $a_p$ value and a predicted $a_p$ value for the next 3-hour period are currently available from Air Force sources. If a running sum of 8 $a_p$'s is maintained, the model can be used to predict the ambient conditions (that is, if

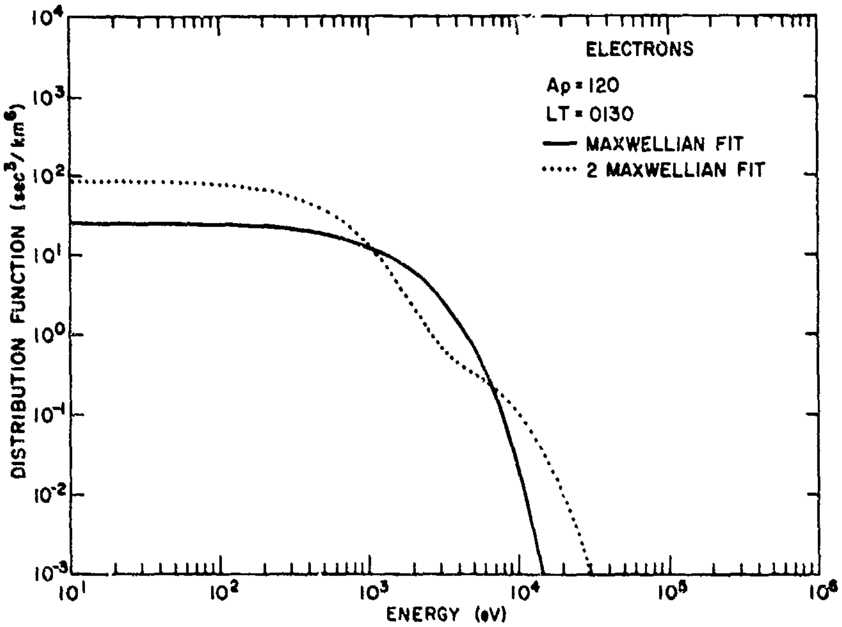


Figure 4. Maxwellian and 2 Maxwellian Electron Distribution Functions Predicted by the Model for $A_p$ of 120 and a Local Time of 0130

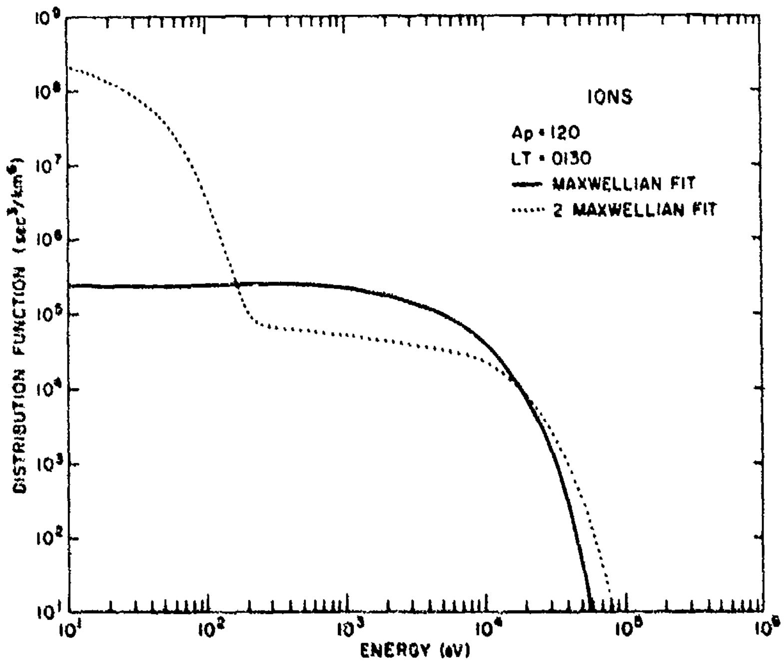


Figure 5. Maxwellian and 2 Maxwellian Ion Distribution Functions Predicted by the Model for $A_p$ of 120 and a Local Time of 0130

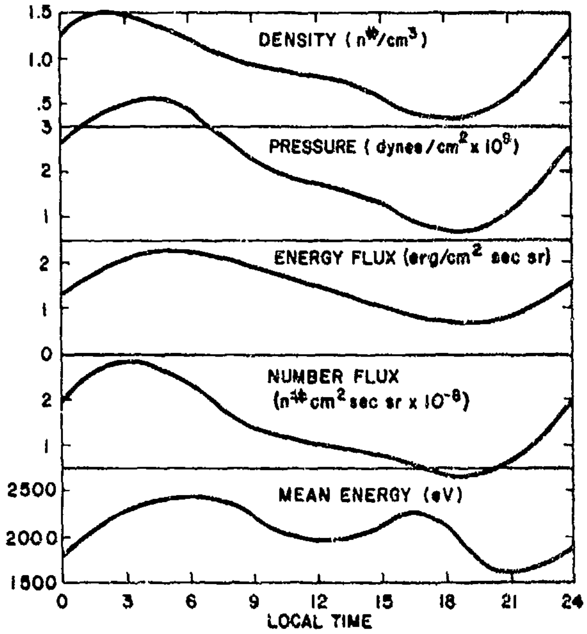


Figure 6. Local Time Plot of the Values of the Four Electron Moments Predicted by the Model for $A_p$ of 120

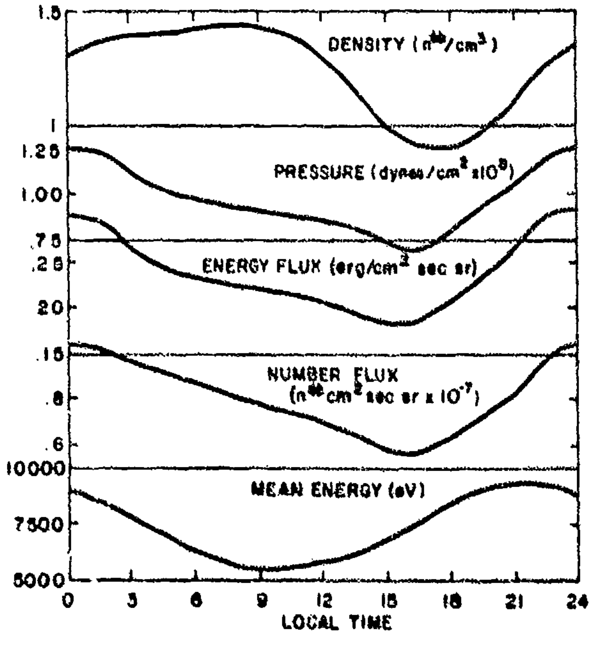


Figure 7. Local Time Plot of the Values of the Four Ion Moments Predicted by the Model for $A_p$ of 120

the preceding 7 $a_p$ values totaled 105 and the predicted $a_p$ was 15, then $A_p$ predicted would be 120 and the environment versus local time for the next three hours would be as shown in Figures 6 and 7). Likewise, if the current $A_p$ value is 120, Figures 6 and 7 illustrate the average conditions following an injection near the local midnight portion of a satellite's orbit, the condition most likely to foster charging. Extreme conditions, suitable for providing a spacecraft charging alert, are estimated by taking the largest observed or predicted $a_p$ value in the desired interval and multiplying by 8 (if the highest $a_p$ was 15, then $A_p$ predicted would be 120). The values so derived can then be inserted in a program that computes spacecraft potential to give an "alert" bulletin versus local time.

## 7. CONCLUSION

In review, we have outlined a procedure for generating an analytic formulation of the various parameters needed by researchers seeking to model the geosynchronous environment and the interaction of that environment with a spacecraft. An environmental model based on a limited data set (10 days) was analyzed under this procedure. The results were compared with other observations of the geosynchronous plasma. Although the model was designed to analyze plasma variations following a plasma injection near the midnight portion of the satellite orbit, excluding anisotropic fluxes and orbital effects, it included geomagnetic and local time variations. Key features of the magnetosphere such as the plasma decrease near evening were reproduced, and various trends in the data which may be significant noted. In view of the assumptions and size of the data base, this model is considered to be a preliminary rather than a definitive description of the ambient geosynchronous environment. As the power of the technique has been demonstrated, it is planned to extend it in the near future to a much more comprehensive data base and, in turn, generate a more complete model.

## References


1. DeForest, S.E. (1972) Spacecraft charging at synchronous orbit, J. Geophys. Res. 77(No. 4):651.
2. McPherson, D.A., Cauffman, D.P., and Schober, W. (1975) Spacecraft Charging at High Altitudes – The SCATHA Program, AIAA paper, pp. pp. 75-92.
3. Pike, C., and Bunn, M.H. (1976) A correlation study relating spacecraft anomalies to environmental data, Spacecraft Charging by Magnetospheric Plasma, AIAA Progress in Astronautics and Aeronautics Series, Vol 42.
4. Garrett, H.B., Pavel, A.L., and Hardy, D.A. (1977) Rapid Variations in Spacecraft Potential, AFGL-TR-77-0132.
5. DeForest, S.E., and McIlwain, C.E. (1971) Plasma clouds in the magnetosphere, J. Geophys. Res. 76(No. 16):3587-3611.
6. Reasoner, D.L., Lennartsson, W., and Chappell, C.R. (1976) Relationship between ATS-6 spacecraft-charging occurrences and warm plasma encounters, Spacecraft Charging by Magnetospheric Plasmas, AIAA Progress in Astronautics and Aeronautics Series, Vol. 42.
7. Stevens, N.J., Lovell, R.R., and Purvis, C.K. (1977) Provisional specification for satellite time in a geomagnetic substorm environment, Proc. of the Spacecraft Charging Conference, AFGL-TR-77-0051/NASA-TMX-73537.
8. Su, S.-Y., and Konradi, A. (1977) Description of the Plasma Environment at Geosynchronous Altitudes, to be published as NASA-Johnson Note P-10.
9. Rostoker, G. (1972) Geomagnetic indices, Rev. Geophys. 10(No. 4):935.
10. Bevington, P.R. (1969) Data Reduction and Error Analysis for the Physical Sciences, McGraw-Hill, New York.
11. Vasyliunas, V.M. (1968) A survey of low energy electrons in the evening sector of the magnetosphere with Ogo 1 and Ogo 3, J. Geophys. Res., 73:2839.

12. McIlwain, C.E. (1971) Plasma convection in the vicinity of the geosynchronous orbit, Earth Magnetospheric Processes, B.M. McCormac, Ed., D. Reidel Publishing Co., Dordrecht, Holland.

13. Mauk, B., and McIlwain, C.E. (1974) Correlation of $K_p$ with the substorm-injected plasma boundary, J. Geophys. Res. 79:3193.

14. Inouye, G.T. (1976) Spacecraft potentials in a substorm environment, AIAA Progress in Astronautics and Aeronautics Series, Vol. 42, pp. 103-120.

15. DeForest, S.E. (1977) Final Report for 1 June 1976–30 November 1976, AFGL-TR-77-0031.

16. Akasofu, S.-I., and Chapman, S. (1972) Solar-Terrestrial Physics, Clarendon Press, Oxford.

# Appendix A

## Calculation of Moments

The ATS-5 UCSD instrument makes measurements only between 51.6 eV and 51.6 keV. Further, all positive ions are assumed to be ionized hydrogen as it is not possible to calculate accurately the composition of the ion population. Thus, the four moments calculated from the ATS-5 data are in actuality valid only for the range 51.6 eV to 51.6 keV for electrons and protons. DeForest[1] notes that the main error introduced by these effects is an underestimation of the particle density and a lack of equality between the proton and electron densities as a large part of the particle population is below 50 eV. With this in mind, the formulas for the moments in Eqs. (5), (6), (7), and (8) are approximated for the electrons by:

$$\langle N_e \rangle = 4\pi \sum_{E_i} \left.\frac{d(EF)}{dE}\right|_i \left(\frac{2E_i}{M_e}\right)^{-1/2} \frac{\Delta E_i}{E_i} \tag{1A}$$

$$\langle NF_e \rangle = \sum_{E_i} \left.\frac{d(EF)}{dE}\right|_i \frac{\Delta E_i}{E_i} \tag{2A}$$

$$\langle P_e \rangle = 4\pi \sum_{E_i} \left( \frac{m_e}{2} \right) \frac{d(EF)}{dE}\bigg|_i \left( \frac{2E_i}{m_e} \right)^{1/2} \frac{\Delta E_i}{E_i} \tag{3A}$$

$$\langle EF_e \rangle = \sum_{E_i} \left( \frac{m_e}{2} \right) \frac{d(EF)}{dE}\bigg|_i \left( \frac{2E_i}{m_e} \right) \frac{\Delta E_i}{E_i} \tag{4A}$$

where

$\sum_{E_i}$ = summation over the energies $E_i$ from 51.6 eV to 51.6 keV

$m_e$ = mass of electron

$\frac{d(EF)}{dE}\Big|_i$ = differential energy flux (count rate divided by $4.3 \times 10^{-5}$ $cm^2$ sr for ATS-5)

$\frac{\Delta E_i}{E_i}$ = 0.12 for ATS-5

The ion moments are similarly derived by replacing $m_e$ by $m_i$, the mass of a proton.

## Appendix B

### Calculation of the 2 Maxwellian Distribution

The distribution function f is of central importance in various schemes for the calculation of spacecraft potential. As Figure 1 clearly demonstrates, a single Maxwellian distribution is often inadequate in describing the actual data. Although a 2 Maxwell fit is also only an approximation, it does double the knowledge of the actual distributions. Further, it tends to divide the particle distribution into two components: a high temperature, relatively low density component and a low temperature, high density component which is consistent with various observations of the actual state of the magnetospheric plasma. For these reasons, to include the calculation of the two densities ($N_1$ and $N_2$) and temperatures ($T_1$ and $T_2$) in the model was warranted.

Assuming a 2 Maxwellian distribution to be given by Eq. (9) and making the additional assumption that the four moments given in Appendix A represent adequate approximation to the actual distribution function, we obtain:

$$N_1 + N_2 = C_1 \tag{5A}$$

$$N_1X_1 + N_2X_2 = C_2 \tag{6A}$$

$$N_1X_1^2 + N_2X_2 = C_3 \tag{7A}$$

$$N_1X_1^3 + N_2X_2^3 = C_4 \tag{8A}$$

where

$N_1, N_2$ = number densities for species i

$X_1 = T_{1i}^{1/2}$, temperature 1 for species i

$X_2 = T_{2i}^{1/2}$, temperature 2 for species i

$C_1 = \langle n_i \rangle$

$C_2 = \langle NF_i \rangle$

$C_3 = \langle P_i \rangle / K$

$C_4 = \langle EF_i \rangle$

Solving:

$$N_1 = C_1 - N_2 \tag{9A}$$

$$N_2 = \frac{C_2 - X_1}{X_2 - X_1} \tag{10A}$$

$$X_2 = \frac{C_3 - C_2 X_1}{C_2 - C_1 X_1} \tag{11A}$$

$$(C_2^2 - C_1 C_3)\, X_1^2 + (C_1 C_4 - C_2 C_3)\, X_1 + (C_3^2 - C_2 C_4) = 0 \tag{12A}$$

Equation (12A) is a quadratic equation and has two roots of the form:

$$X_1 = \frac{-B + \sqrt{B^2 - 4AC}}{2A} \tag{13A}$$

$$X_1 = \frac{-B - \sqrt{B^2 - 4AC}}{2A} \tag{14A}$$

where

$A = C_2^2 - C_1 C_3$

$B = C_1 C_4 - C_2 C_3$

$C = C_3^2 - C_2 C_4$

This situation may appear ambiguous, but it is obvious by the symmetry of Eqs. (5A), (6A), (7A), and (8A) that if we choose the positive sign for $X_1$, then $X_2$ must correspond to the negative sign. The actual problem is that it is possible that the distribution function is a single Maxwellian in which case $X_2$ (or by symmetry, $X_1$) will approach infinity and the number density, $N_2$, zero. Some care must be exercised in studying trends as a result of this effect.

For actual data, it is not likely that imaginary or negative values will be encountered. For values derived from our simple model, this is not true: The fitted moments may be negative (in which case imaginary values are obtained), or the minimum correction values may result in negative densities. Fortunately, this happened for only 7 of the 80 values calculated for the electrons; it did not occur for the ions. Default values representative of the expected minimum values are returned by the program in these cases (see Appendix C). Finally, $T_{1i}^{1/2}$ or $T_{2i}^{1/2}$ may be negative and should be checked in any general application.

# Appendix C

## FORTRAN Listing of Environmental Model

The model outlined in this study consists of two subroutines: MODEL and MAXW. These two programs have separate purposes and can, with minor changes, be used independently.

Subroutine MODEL requires as input the daily $A_p$ index and the local time LT (a real number). It returns a vector XX which has the 20 components:

XX(1) = Electron density × 100 (number/$cm^3$)

XX(2) = Ion density × 100 (number/$cm^3$)

XX(3) = Electron pressure × $10^{10}$ (dynes/$cm^2$)

XX(4) = Ion pressure × $10^{10}$ (dynes/$cm^2$)

XX(5) = Electron energy flux × 100 (erg/$cm^2$ sec-sr)

XX(6) = Ion energy flux × 100 (erg/$cm^2$ sec-sr)

XX(7) = Electron number flux × $10^{-6}$ (number/$cm^2$ sec-sr)

XX(8) = Ion number flux × $10^{-6}$ (number/$cm^2$ sec-sr)

XX(9) = Electron mean energy (eV)*

XX(10) = Ion mean energy (eV)*

---

*Mean energy, which is 3/2 KT for a Maxwellian, should not be confused with the temperature, KT, used in generating the Maxwellian or 2 Maxwellian distribution.



PRECEDING PAGE BLANK-NOT FILMED

XX(11) = Electron current $\times 10^4$ (n amps/cm$^2$)

XX(12) = Ion current $\times 10^4$ (n amps/cm$^2$)

XX(13) = Electron density 1 $\times$ 100 (number/cm$^3$)

XX(14) = Ion density 1 $\times$ 100 (number/cm$^3$)

XX(15) = Electron temperature 1 (eV)

XX(16) = Ion temperature 1 (eV)

XX(17) = Electron density 2 $\times$ 100 (number/cm$^3$)

XX(18) = Ion density 2 $\times$ 100 (number/cm$^3$)

XX(19) = Electron temperature 2 (eV)

XX(20) = Ion temperature 2 (eV)

Subroutine MODEL requires MAXW but it can easily be deleted if the 2 Maxwellian distribution is not required. Subroutine MAXW requires a set of four moments:

RHO = density (number/cm$^3$)

FNO = number flux (number/cm$^2$-sec-sr)

PR = pressure (dynes/cm$^2$)

FEN = energy flux (erg/cm$^2$-sec-sr)

A value of 1 is used for electrons, 2 for ions. It returns:

R1 = density 1 (number/cm$^3$)

Y = temperature 1 (eV)

R2 = density 2 (number/cm$^3$)

T = temperature 2 (eV)

These values can be used in Eq. (9) to give an approximation to the distribution function.

Table 2 of the main report gives default values returned by the program. These are the most reasonable estimates of these values that could be determined.

```
      SUBROUTINE MODEL(AP,LT,XX)
      DIMENSION XMIN( 8),X(10, 8),XX(20)
      REAL LT
      DATA ((X(I,J),I=1,10),J=1,8 )/
     1  .3835E+02,-.4166E+02, .2184E+02,-.2101E+01,-.2312E+02,
     1  .4255E+00,-.7337E-01,-.5953E-01,-.8028E-01, .4436E-01,
     1  .9853E+02,-.2720E+02, .2276E+01,-.2758E+01,-.3287E+01,
     1  .2980E+00, .9757E-02,-.3543E-01,-.4836E-01, .3773E-01,
     1  .5195E+01,-.1036E+02, .6420E+01, .2609E+01,-.4776E+01,
     1  .1253E+00,-.2784E-01,-.3329E-01,-.2031E-01, .2257E-02,
     1  .7684E+02,-.4464E+01, .1610E+02,-.8089E+00,-.3110E+01,
     1  .1608E+00,-.4948E-01, .4189E-01,-.6374E-01, .2369E-01,
     1  .3573E+02,-.7375E+02, .5046E+02, .2135E+02,-.1075E+02,
     1  .9136E+00,-.3251E-01,-.5064E+00,-.1706E+00,-.4715E-01,
     1  .1858E+02,-.5158E+00, .3109E+01,-.6267E-01,-.8042E+00,
     1  .3776E-01,-.1237E-01, .1490E-01,-.1782E-01, .3398E-02,
     1  .4719E+02,-.6769E+02, .3818E+02, .7563E+01,-.4420E+02,
     1  .0103E+00,-.2435E+00,-.4471E-01,-.1089E+00, .5030E-01,
     1  .6232E+01,-.9452E+00, .1427E+01,-.1282E+00,-.3029E+00,
     1  .1478E-01,-.3372E-02, .7584E-03,-.4736E-02, .2516E-02/
      DATA(XMIN(I),I=1, 8)/2.0,33.,.4,40.,8.,9.,4.,3./
      FLAG=0
      DO 2 I=1,8
      XX(I)=0
      DO 1 J=1,9
      IPA=J/5
      IPT=J-5*IPA
      Y=1
      X1=(LT+6.5)/3.
      TPI=6.28318
      IF(IPT.EQ.1)Y=COS(X1*TPI/8.)
      IF(IPT.EQ.2)Y=SIN(X1*TPI/8.)
      IF(IPT.EQ.3)Y=COS(X1*TPI/4.)
      IF(IPT.EQ.4)Y=SIN(X1*TPI/4.)
      J1=J+1
    1 XX(I)=(AP**IPA)*Y*X(J1,I)+XX(I)
      XX(I)=XX(I)+X(1,I)
      IF(XX(I ).LT.XMIN(I)) FLAG=1
    2 IF(XX(I).LT.XMIN(I)) XX(I)=XMIN(I)
      XX( 9)=XX(3)*9360./XX(1)
      XX(10)=XX(4)*9360./XX(2)
      XX(11)=XX(7)*1.6*3.14159
      XX(12)=XX(8)*1.6*3.14159
      DO 3 I=1,2
      K=I-1
      RHO=XX(K+1)/100.
      FNO=XX(K+7)*1.E+06
      PR=XX(K+3)/1.0E+10
      FEN=XX(K+5)/100.
      CALL MAXM(RHO,FNO,PR,FEN,A,B,C,D,I)
      XX(K+13)=A*100.
      XX(K+15)=B
      XX(K+17)=C*100.
    3 XX(K+19)=D
      IF(XX(15).LT.200.)GO TO 5
      IF(FLAG.EQ.0.0) GO TO 4
```

```
    5 XX(9)=1000
      XX(13)=XX(1)
      XX(15)=.25).
      XX(17)=XX(1)/50.
      XX(19)=2*000
    4 CONTINUE
      RETURN
      END
```

```
      SUBROUTINE MAXW(RHO,FNO,PR,FEN,R1,Y,R2,T,I)
C     I=1 IS FOR ELECTRONS.  I=2 IS FOR IONS
      DIMENSION X(2),Z(2)
      X(1)=2.022E-05
      X(2)=8.05E-04
      Z(1)=7.32E+10
      Z(2)=3.14E+12
  100 FORMAT(4(1X,E13.6))
  101 FORMAT(1X,*IMAGINARY*)
      C1=RHO
      C2=FNO*X(I)
      C3=PR/1.38E-16
      C4=FEN*Z(I)
      A=C2*C2-C1*C3
      B=C1*C4-C2*C3
      C=C3*C3-C2*C4
      D=B*B-4.*A*C
C     CHECKS FOR IMAGINARY ROOT
      IF(D.LT.0.0) GO TO 99
      Y=((-B+SQRT(D))/(2.*A))
C    CHECKS FOR PROPER ROOTS
      G=((-B-SQRT(D))/(2.*A))
      T=(C3-C2*Y)/(C2-C1*Y)
      IF(ABS(T-  ).LT..01    ) GO TO 98
      PRINT 100,Y,T,G
   98 CONTINUE
      R2=(C2-Y*C1)/(T-Y)
      R1=C1-R2
      Y=Y*Y/1.15E+04
      T=T*T/1.15E+04
      G=G*G/1.15E+04
      RETURN
   99 PRINT 101
      PRINT 100,A,B,C,C1,C2,C3,C4
      A=B=C=D=3
      END
```